The neuronal basis of spontaneous flight behavior in *Drosophila*

Inaugural-Dissertation to obtain the academic degree Doctor rerum naturalium (Dr. rer. nat.)

submitted to the Department of Biology, Chemistry and Pharmacy of Freie Universität Berlin

by

Sathishkumar Raja

From Namakkal 11°13′N 78°10′E

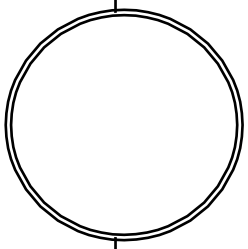

May, 2013

Ph.D. Dissertation Supervisor – Dr. Björn Brembs,

Institut für Biologie - Neurobiologie,

Freie Universität Berlin.

2010 – 2013.

1st Reviewer: Prof. Dr. Björn Brembs

2nd Reviewer: Prof. Dr. Hans-Joachim Pflüger

Date of defence: 13/06/2013

DEDICATED TO TRUE FLIES....

TABLE OF CONTENTS:

1 INTRODUCTION

Brain function is primarily studied by observing correlations between behaviors and environmental events. Behavioral responses are considered to be stereotypic patterns of reflexes driven by immediate environmental stimuli. This view can be traced to the early work of Sherrington (Burke, 2007; Levine, 2007; Sherrington, Charles Scott, Sir, 1920), who emphasized the role of sensory inputs on reflexive behavior. This finding stimulated a number of studies, on animals from single cell organisms (Jimenez-Sanchez, 2012) to humans (Churchland et al., 2010; Müller et al., 2013; Sommer et al., 2013), that were designed on the assumption that external cues elicit appropriate responses or, stated another way, that brain function is best understood in terms of input-output transformations (Borst & Egelhaaf, 1989; Borst & Bahde, 1988; Dickinson et. al 2013; Huston & Jayaraman, 2011; Maimon & Dickinson, 2010; Murray & Wallace, 2011; Wessnitzer & Webb, 2006).

For example, behavioral studies of insects are conducted by manipulating various stimuli that are known to cause behavioral responses. Insects have several sensory modalities that receive external cues and relay relevant information to central processing circuits for successful motor output (Dickinson, 2005; Frye & Dickinson, 2004). The major sensory modalities of insects are olfaction, taste, mechanoreception and vision. These have been studied extensively using behavioral, genetic and neurophysiological methods. (Frye et al., 2011; Götz, 1987; Borst et al., 2011; Nachtigall & Wilson, 1967; Renn et al., 1999). This behavioral research illuminates brain function by focusing on the neural mechanisms of insects that process sensory stimuli to produce complex behaviors (Comer & Robertson, 2001; Renn et al., 1999; Strauss, 2002; Venken, Simpson, & Bellen, 2011).

1.1 Neuronal basis of visually guided behaviors

Most of the behavioral studies of insect flight have been conducted by presenting visual stimuli in the form of gratings (Borst & Bahde, 1988; Tammero & Dickinson, 2002). Flies are better able to abstract fast-moving stimuli than many other species. Tethered flight studies are conducted in a flight simulator where the flies are partially immobilized in the center of a panorama on which visual cues are projected (Götz, 1968; Frye et al., 2008; Wang et al., 2008; Wolf & Heisenberg, 1980; Reinhard Wolf & Heisenberg, 1991). Studies involving free and tethered flight have successfully addressed the underlying neuronal processes governing visual-motor transformation during such events as obstacle avoidance (Horridge, 2009; May, 2012), object discrimination (Borst & Egelhaaf, 1989; Comer & Robertson, 2001; Griffith, 2012) and escape behavior (Card & Dickinson, 2008; Conner & Corcoran, 2012; Dewell & Gabbiani, 2012; Domenici, Blagburn, & Bacon, 2011; Roeder, 1962). These studies have shown that a visual cue that reaches the visual system is encoded, processed through central circuitries, integrated by mechanosensory feedback, and finally transformed into a specific flight maneuver (Borst & Haag, 2002; Frye & Dickinson, 2004). The pathways that route visual information toward descending interneurons have been studied extensively (Borst & Egelhaaf, 1989; Borst & Reiff, 2010; Borst, 2009; Collett, 2002; Götz, 1968; Jung et al., 2011; Gong & Liu, 2012). These descending interneurons are believed to carry stimulus information from sensory units that is essential for flight motor circuitry (Maimon et al., 2010). However, the mechanism involved in triggering motor patterns by central circuitry is largely unstudied.

It has been shown that fast-moving cues are recognized by a set of wide- and small-field neurons. These neurons are specialized cells that detect the direction of motion and the movement of a small object against its background (Card & Dickinson, 2008; Borst, & Haag, 2005). A pair of large-diameter interneurons, known as giant fibers, mediate the fast motor responses that initiate fly escape sequences (Card & Dickinson, 2008; Wyman, 2013). The relationship between

identified neurons and behavior is ultimately established by observing sensory-motor processing. Such findings support the assumption that control of the motor units involved in any flight behavior is stimulus-regulated and eliminate the possibility of endogenously generated motor actions.

1.2 Neuronal causes for spontaneous behavioral variability

1.2.1 Spontaneous occurrence of animal behavior and its variability

Spontaneous behavior is ubiquitous in several biological systems (Miller, 1997; April, 1970). The movement dynamics of many animals show relatively variable and spontaneous behavior. The copepod *Temora longicornis* Müller is a small crustacean that floats on water and feeds on unicellular algae. Copepods initiate movement toward the algal rich zone, but when they are reared in a lab environment providing no algae in the water, they travel in a straight line with interspersed spontaneous quick turns (Schmitt & Seuront, 2001). This is considered to be a spontaneous exploratory movement. The giant water bug *Belostoma flumineum* displays alternation between left and right turns in a T-maze in a seemingly random fashion. Goldfish switch between a slow and quick swimming pattern in a uniform visual environment. Most importantly, the duration of the activity is variable (Nepomnyashchikh, 2013).

1.2.2 Variability in behavior is an adaptive trait

Spontaneous behavior generated by animals is highly variable (Maye et al., 2007; Nepomnyashchikh & Podgornyj, 2003). It is therefore difficult to predict every move that an animal will make. It has been suggested that brains have evolved over time to generate unpredictable adaptive variability in behaviors such as those involved in competition, courtship and chasing (Nepomnyashchikh & Podgornyj, 2003; Nepomnyashchikh, 2013; Wilkinson, 1997). This view began with the 'Machiavellian Intelligence' hypothesis, which states that animals and humans developed specific cognitive skills for predicting and manipulating the actions of other beings. Individuals have developed a protean strategy to prevent other

animals from successfully predicting their behavior (Miller, 1997; April, 1970). Behavior that is unpredictable favors survival and is thus adaptive. These unpredictability strategies were first identified in the 1960s, in studies of the escape strategies of moths and the facultative defensive behaviors of rats (Chance, 1957). Moths execute combinations of loops, rolls, and dives to evade bats (Roeder, 1964; Roeder, 1962). Rats randomly exhibit convulsions upon hearing noxious tones. These behaviors would confound a predator and make it more difficult for it to catch prey. If animals actions were automata, every action would be released by a stimulus that determines behavior (Wilkinson, 1997).

These examples of predator-prey interaction show that unpredictable behavior is certainly advantageous for survival. Consistency in stereotyped predator avoidance responses would make prey more vulnerable. Unpredictability is not limited to predator-prey interactions. Variability also maintains orderly behavior at several levels of animal organization. Some examples are posture maintenance (Oullier, Marin, & Stoffregen, 2006), landing on objects (Saint-germain, Drapeau, & Buddle, 2009) and perceptual scanning (Estes, 1965). Variability is utilized at several levels of physiological organization. Complex behavioral repertoires are developed by reinforcement of behavioral variants, for example in random exploratory behavior (Miller, 1997). Nevertheless, unpredictability is observed in animal actions, movement signals, and social interactions. However, variability could be highly disadvantageous if it is entirely randomly generated. Prey could be falling directly on top of a predator during truly random predator avoidance.

1.2.3 Intrinsic neuronal properties for spontaneous variability

Evolution is largely assumed to produce deterministic mechanisms of animal behavior. Unpredictability is disregarded as a noisy component according to the computational principles of the input-output hypothesis (Selen & Wolpert, 2008; Series & Note, 2000; Gossen, & Jones, 2005). The sensorimotor integration principle also does not provide a sufficient interpretation of the spontaneous behavioral variability that occurs in a wide range of species. Brain functions are complex, and

studies of sensorimotor integration have not produced a complete picture of brain function. To the best of our knowledge of brain structure, function arises through the transmission of information from sensory to motor networks. Variability thus does not arise from completely random or chance components in the brain. The combination of inevitability (e.g., primary goal, escape) and variability favors unpredictable behavior. The precision of the required behavior is largely dependent on the needs of an animal in a particular environment. Neuronal circuits in the fly brain are proposed to mediate such organized behavioral architecture (Maye et al., 2007).

In higher-order brain systems, spontaneous activity occurs at the neuronal level (Andrews-Hanna et al., 2008; He et al., 2010; Proekt, Banavar, Maritan, & Pfaff, 2012; Raichle, 2010). Variability in the timing of evoked neuronal spiking is reported as well. This variability in the timing of neuronal firing is associated with spontaneous brain activity. Specific neuronal networks called default mode networks (DMNs) have been shown to interact and thus induce brain activity (Raichle, 2010). This interaction is a primary cause for variability in the human brain. However, a direct comparison with invertebrate brain structures is not productive given the huge gap in brain complexity. However, *Drosophila* and humans share certain brain properties, as evidenced by similarities in mediating action selection and time allocation by the insect and human brains (Van Alphen, & Pierre, 2010; Reiter & Bier, 2002).

Maye et al., 2007 proposed a neuronal cause for spontaneous variability after investigating the temporal structure of behavioral variability in *Drosophila*. Restrained *Drosophila* can spontaneously produce yaw torques in a flight simulator with no visual cues that could potentially elicit turning responses (Maye et al., 2007; Wolf and Heisenberg, 1984). The yaw torque generated spontaneously by the flies is highly variable, with random alternation between left and right turns. These actions are proposed to be dependent on active and voluntary brain activities (Maye et al., 2007). The interval between alternating turns shows a fractal order

resembling levy flights, suggesting the role of initiation by an endogenous neuronal entity(ies). This endogenous neuronal entity is proposed to act as a deterministic system to keep variability under neural control.

The few studies of endogenous animal behavior highlight some yet-unanswered ultimate questions, such as 'Is there a neural entity mediating such processes with negligible external cues?' and 'If so, how is the endogenous generation of spontaneous variability in *Drosophila* organized without external input?'

1.3 Neuroethological approach to neuronal circuit investigation

1.3.1 Endogenous flight behavior of *Drosophila* as measured by a wing beat analyzer

In general, measuring endogenously generated motor output is required for finding the neuronal causes of spontaneous behavior. External cues should have minimal or no influence over the measured output. Flight simulators have been used for several decades to measure visual-motor responses in a controlled environment. Flight simulators have been used widely to study such topics as visual motion detection, visual learning, orientation, reafference controls, and optomotor responses (Brembs, 2002; Liu et al., 2006; Wolf & Heisenberg, 1991). Display systems that are based on light-emitting diodes (LEDs) (Reiser & Dickinson, 2008) have recently been used to display panoramic visual motion at high spatial and temporal resolution. The inter-ommatidial distance of the *Drosophila* eye is more than the individual pixel size of an LED display unit (Chow et al., 2011; Mamiya & Dickinson, 2011; Reiser et al., 2011). The fly retina is thus able to detect any minute spatial movement in an arena. For spontaneous behavioral studies, flies are tethered and the flight arena is programmed to display a uniform, unchanging display environment. The feedback loop between the behavior and the environment is open. This uniform environment is suitable for measuring endogenous flight behavior because it excludes external stimuli. *Drosophila* can fly under these

conditions, and the wing beat amplitude is measured for computing yaw torque. Tethering also limits the fly's mobility, but this procedure offers several advantages in addition to environmental control. For example, because the tethered flies have no spatial movement, there can be no angular rotation feedback to the flight motor center such as that from halters (Chow et al., 2011; Huston & Krapp, 2009; Sherman, 2003).

The electronic visual flight arena and the wing beat analyzer have proven to constitute a suitable system for delivering controlled visual stimuli and measuring yaw torque motor output (Dickinson, 2005; Dickinson, 1993; Reiser & Dickinson, 2008). The optical sensor-based wing beat analyzer measures the wing beat amplitudes of individual wings. The left and right wing beat amplitude difference is equivalent to a yaw saccade turn detected during free flight. This yaw torque measurement under homogenous spatial scenery is used as a measure of endogenous motor output production. Therefore, yaw turning actions generated by the flies are not triggered by visual cues, and any modulation in yaw turning originates intrinsically from the fly brain.

1.3.2 Dissection of neuronal circuits using the Gal4-UAS system coupled with a tetanus toxin light chain (TeTxLC):

A noninvasive targeted expression tool known as the Gal4-UAS tool system is widely used to identify the causal neuronal bases of a specific behavior (Duffy, 2002; Martin & Sweeney, 2002; Renn et al., 1999; Venken et al., 2011). The basic concept of this system is accessing a behavioral function in the absence of a specified neuronal population to determine the causal circuitries by elimination. This system allows the expression of a gene of interest in any neuronal cell or group of tissues. For example, the tetanus toxin light chain (TeTxLC) is widely used to investigate the role of a particular brain region on a specific behavior. The usefulness of this approach is due to the mechanism and action of the tetanus toxin light chain. The light chain inhibits exocytotic neurotransmitter release by proteolytically cleaving a protein called synaptobrevin. Synaptobrevin (Sweeney et al., 1995) is found to

interact with presynaptic proteins to mediate an evoked transmitter release by effectively silencing the neuronal region affected by this toxin. This concept has led to the identification and molecular characterization of several neuronal bases and associated pathways in olfaction, mechanoreception, higher order locomotion and vision in fruit flies.

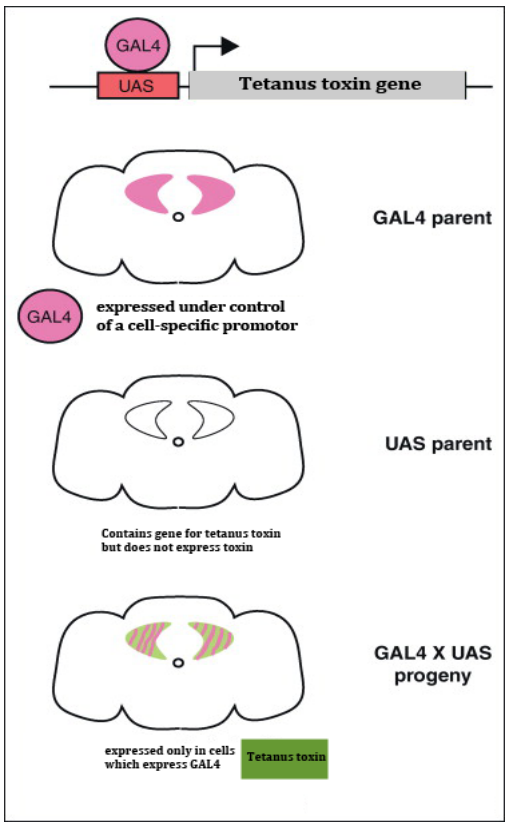

Fig. 1. The Gal4-UAS system.

This figure depicts the working principles of Gal4-UAS system. Effector lines consist of a Gal4-binding upstream activation sequence (UAS) with the sequence of the gene of interest (tetanus toxin gene). In UAS-TNT-E flies, the tetanus toxin light chain gene is placed next to UAS elements. The toxin is only expressed in cells of the progeny that express Gal4 (adapted from Griffith, 2012).

The Gal4-UAS system is used to express tetanus toxin into the neural cells. Gal4 is a transcriptional activator protein that activates transcription in the yeast *Saccharomyces cerevisiae* induced by galactose. Gal4 directly binds to a defined site, called the "Upstream Activating Sequence" (UAS) and has no target in the fly genome. The tool uses a transposable "P-element" construct that can be inserted into the fly genome at different sites. The P-element contains the Gal4 sequence

with either a known promoter (promoter-fused Gal4 lines) or a weak promoter that will "trap" enhancers close to the insertion site (enhancer trap line) (Brand & Perrimon, 1993). GAL4, in turn, directs the transcription of the GAL4-responsive UAS target gene in an identical pattern. This bipartite approach, which uses two separate parental lines, i.e., the driver (Gal4) line and the effector (UAS) line, has a major advantage: the ability to target the expression of any effector gene in a variety of spatial and temporal ways by crossing it to distinct Gal4 drivers. Wide ranges of Gal4 driver fly lines are available commercially with expression patterns ranging from a group of cells to entire brain regions.

1.3.3 A dynamic systems approach for investigating neuronal circuits

There is spontaneity in a given system that is independent of the stimulus. A stimulus-behavior unit is a deterministic linear system when a sensory stimulus triggers central circuitries and directly facilitates the resulting behavior. However, spontaneity is manifested in a nonlinear dynamic system. The system with spontaneous behavior is said to be a nonlinear dynamic system because the behavioral actions are not specifically proportional to the external sensory parameters. This endogenously generated behavior could have an unpredictable or deterministic nature and reflects the nonlinear nature of the system (Abarbanel & Rabinovich, 2001; Nepomnyashchikh & Podgornyj, 2003; Sugihara & Mayf, 1990; Wilkinson, 1997). The internal nonlinear circuits of the system modulate the variability in the spontaneous behavior (Maye et al., 2007).

For example, flies generate unpredictable behavior in the torque meter under a uniform visual environment (Maye et al., 2007). This system of behavior generation without any external input implies a nonlinear system. The behavioral actions of the flies are computationally unpredictable but are initiated by an intrinsic neuronal process. However, the neural circuits act as a deterministic system to mediate the behavioral variability. Nonlinear prediction tools such as S-Map analysis (Maye et al., 2007; Sugihara & Mayf, 1990) are available to categorize

the properties of a system to help understand the nature and origin of behavioral actions.

If external factors do not trigger intrinsic spontaneous processes, the system can be perturbed according to dynamic laws (Wilkinson, 1997). In other words, external cues could only perturb but not trigger the processes (neurons) that produce stimulus-oriented behaviors. The nonlinear nature of the system thus involves the role of neuronal circuitries in modulating given behavioral actions. As an ideal example, bacteria actively move in one direction and turn sharply in different directions when they perceive a chemical stimulus (Griffith et al., 2012; Jimenez-Sanchez, 2012). The stimulus immediately alters the behavior, and the organism moves away from the chemical stimulus. The neuronal components (nonlinear structures) mediating spontaneous turns are quantitatively altered and stimulate behavior that is more suited to the external situation.

1.4 A strategy to establish the link between a neuronal circuit and spontaneous behavioral generation

The strategies employed in this study to elucidate the neural circuits for spontaneous behavioral variability are explained below. The ultimate aim is to use genetic and mathematical tools to identify the neuronal structures involved in spontaneous yaw turning behavior in *Drosophila*. The central focus of this study is a behavior called spontaneous yaw torque behavior. It was essential to provide a detailed description of this behavior, including the environmental conditions under which the fly generates the behavior. We had to acquire instrumentation to measure the behavior and identify any other variables that are necessary to describe the behavior. Much of the information on the properties of spontaneous variability was obtained from the study of Maye et al., 2007. After describing the characteristics of the behavior in detail, we attempted to identify the circuits involved in the spontaneous behavior by measuring the spontaneous yaw turning behavior of various transgenic flies and screening for linear temporal properties

using the S-Map procedure. The major advantage of the *Drosophila* model is the ability of the Gal4-UAS genetic tool system to silence different brain regions. Gal4 fly lines are readily available (Jenett et al., 2012), with a wide range of expression patterns covering different parts of the fly brain. The screening procedure involves using the results from the S-Map analysis to find candidate fly lines that do not show the nonlinear signature that is observed in wild type flies. The yaw turning actions had to be measured under the uniform visual environment that is produced by the previously validated combination of an LED-based flight arena and a wing beat analyzer.

Specific neuronal structures are recognized as necessary for spontaneous yaw torque behavior when disturbance of the structures changes the behavior's temporal properties. The effects of circuit ablation on behaviors such as walking and flight also allow better understanding of circuit function. Descriptors of the neural circuitries are important for understanding the crucial functional role of these circuits. A simplified approach would involve the characterization of behaviors associated with the circuits in transgenic animals. Because variability is observed in flight measures, a logical step would be to assess the candidate fly lines' motor abilities to generate invariable yaw torque maneuvers. Walking competence can concomitantly be measured to link general locomotor function to the circuits that generate variability. A reliable repertoire of spontaneous behavioral properties can be established by evaluating and implementing behavioral data from a candidate line.

2. MATERIALS AND METHODS

2.1 Flies

All flies used in the experiments were raised on a standard cornmeal/molasses/agar medium, on a 12-/12-hour light and dark cycle at 25°C with 60% humidity. The transgenic fly lines used in the experiments, with their respective flybaseID, were c819-Gal4 (FBti0018454), 210y-Gal4 (FBti0004605), MB247-Gal4 (FBtp0012869), c105-Gal4 (FBti0018459), 078y-Gal4 (FBti0015362), 007y-Gal4 (FBti0015361), and c232-Gal4 (FBti0002929).

The UAS-TNT-E line (FBtp0001264) was used to express the tetanus toxin light chain in the Gal4 lines. Wild type Berlin (WTB) flies were used as a control group during the screening procedure. A web resource (http://www.virtualflybrain.org) known as "virtual fly brain" was used to gather information on expression data for the Gal4 fly lines.

P[Gal4] line	Expression pattern
C819-Gal4	Ellipsoid body ring neuron R2 & R4, pars intercerebralis and large field neurons.
210y-Gal4	Fan shaped body, Protocerebral bridge, median bundle, nodulus, subesophageal ganglion, mushroom body and lobula complex.
mb247-Gal4	Mushroom body alpha, beta and gamma-lobes.
C105-Gal4	Ellipsoid body ring neuron R1.
78y-Gal4	Pb-eb-no neuron, small field neuron, pars intercerebralis, ellipsoid body, Protocerebral bridge and nodulus.
007y-Gal4	Ellipsoid body, nodulus, small field neurons, pb-eb-no neurons and Protocerebral bridge, K.C.
C232-Gal4	Ellipsoid body ring neuron R3 & R4d.

2.2 Spontaneous yaw torque measurement

2.2.1 Tethering flies for yaw torque measurements

Female flies were collected at an age of 24-48 h for the tethering procedure. An individual fly was cold anesthetized briefly in a cold chamber, and a V-shaped tungsten rod (length ~4 mm) was glued between the head and thorax using a dental cure IR-sensitive adhesive (Locktite UV glass glue, Henkel Ltd, HP2 4RQ, United Kingdom). The rod was glued perpendicularly to the longitudinal axis of the fly. Flies were transferred after gluing to a small container containing sugar pellets. These small containers were kept overnight with a continuously moisturized filter paper in an environmentally controlled chamber.

2.2.2 Optical wing-beat analyzer

Wing-beat analyzer equipment (purchased from the James Franck Institute, University of Chicago, USA) was used to measure characteristics of the wing stroke during the flight of a tethered *Drosophila* in real time. The wing-beat frequency and amplitude of each wing was measured. The difference in the wing-beat amplitudes of the two wings was used to calculate the fly's yaw torque (Götz, 1987; Theobald, Duistermars, Ringach, & Frye, 2008).

Hardware component setup

The wing-beat analyzer consisted of a main circuit unit, a photosensor and an infrared LED unit (Fig. 1). Each fly was tethered to a tungsten rod and placed inside the arena such that its pitch angle was 45° from the vertical plane. An infrared light-emitting diode (IR-LED HSDL-4230, Conrad Electronics, Schloßstraße 34-36, Berlin, Germany) with an emission peak at 875 nm was placed above the fly.

The photosensor unit was placed under the fly. It consisted of two infrared-sensitive silicon wafers, placed so that the shadow of one wing would be recorded by one sensor and the shadow of the other wing would be recorded by the other sensor.

Each sensor was connected to an adjustable current amplifier. A crescent-shaped cutaway mask was positioned above the photosensor (Fig. 2). A wavelength-specific visible light attenuator (400-700 nm, FWHM 400 nm, Filcom Photomask Inc. Japan) was kept above this mask to ensure that only the light from the IR LED reached the sensor.

The relative position of a fly was calibrated by moving the fly holder using a micromanipulator, such that the shadow caused by the wing fell on the cutaway mask. The size of the shadow was adjusted by moving the fly and the IR-LED so the shadow was laterally centered over the cutaway mask (Fig. 2). The mask and amplifier ensured that the final output was proportional to the position of the shadow cast by the beating wing. The output voltage represented the shadow of the wing beat, which increased during the forward excursion of the wing.

The photosensor unit transmitted a current proportional to the shadow of the wing, which was not blocked by the mask. These analog signals were filtered with a low pass filter (LPF) with the LPF cut-off set to 1 KHz. The main unit calculated the frequency and the amplitude of individual wing beats. Finally, the calculated wing beat amplitudes were routed to the output connectors.

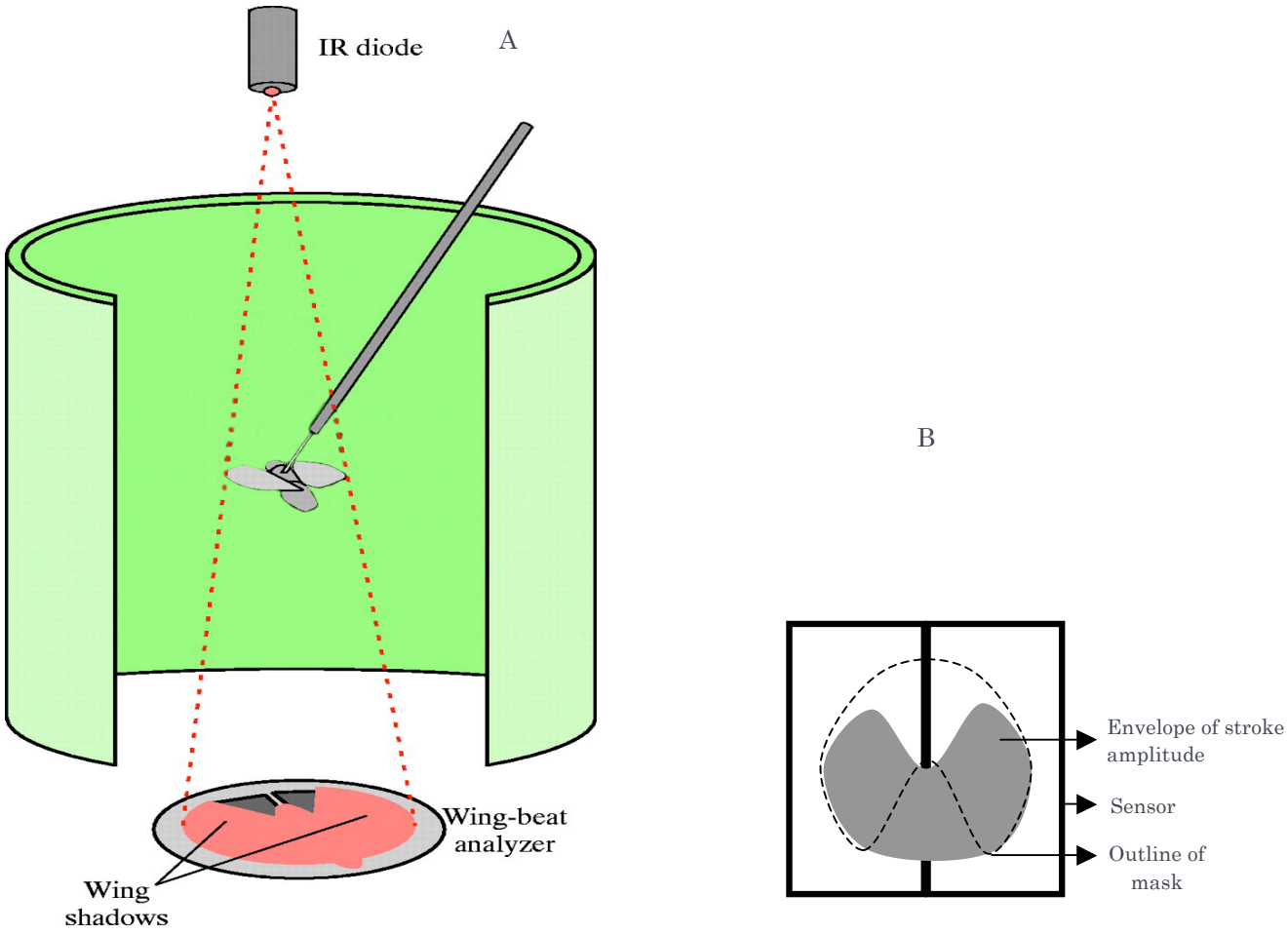

Fig. 2. Schematics of the wing-beat analyzer experimental setup.

A. A tethered fly was placed in a hovering position inside the flight arena. Each fly's wing stroke amplitude was measured by optically tracking the wing shadows cast by the infrared LED. Yaw turning was calculated by subtracting the wing-beat amplitudes of the left and right wings. B. Alignment of the wing shadow (striped area) over the cutaway mask (grey area). The shadow cast by the wings was laterally centered over the cutaway mask.

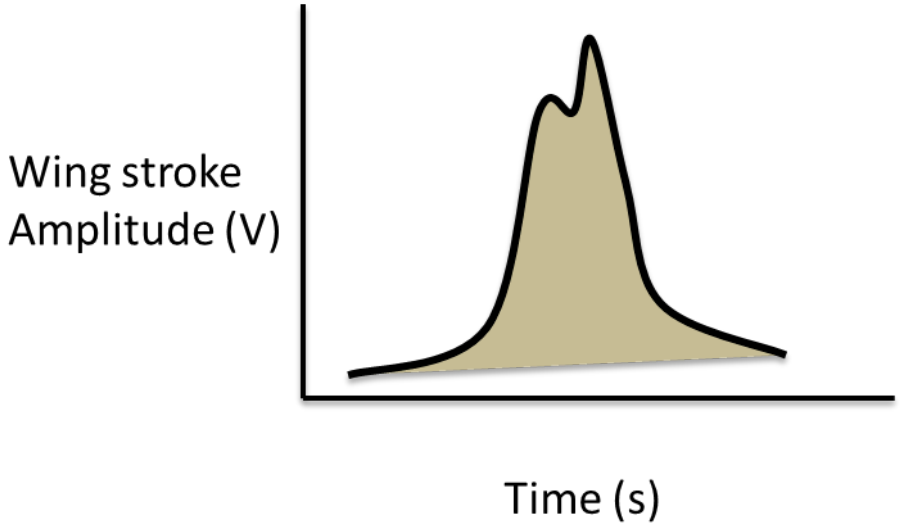

Fig. 3. Typical wing-beat signal obtained from the wing beat analyzer.

Plotted are the two peaks that represent the downstroke and upstroke of an individual wing during a single wing stroke. The larger peak is followed by a smaller peak (Source: JFI electronic laboratory, Chicago).

Inputs to wing beat analyzer equipment

The gain level was adjusted to produce 4 V at the final amplitude signal from the signal-out connectors. Flip excursion was set to 1.5 ms. The gating pulse widths R2 and R29 were set to 1.2 ms for the left and right channels. A source was selected from left or right to set the gating level. The low-pass filter (LPF) cut-off was adjusted to 1 kHz, fine gain to 0.2, coarse gain to 100, trigger lever to 0.40 and gate width to 9.8. The potentiometer in the sensor was adjusted to a unit gain of 5 out of 11.

2.2.3 Signal optimization

The photocurrents obtained from the sensors were transmitted to the main unit to calculate the frequency and amplitude of the wing stroke. The end analog signals corresponding to the calculated yaw torque were converted to computer-readable digital signals using a sampling frequency of 250 Hz. Converter equipment with 12-bit successive approximation (ADC-USB-120FS, Measurement Computing

Inc., USA) was purchased for analog-to-digital data conversion. These converted digital signals were reformulated by employing a moving average filter in MATLAB software (MATLAB 2011a, version 7.12.0, MathWorks Corporation, USA.). The following equation was applied to govern the filtering strategy, used with an averaging factor (M) of 13:

$$y[i] = \frac{1}{M} \sum_{j=0}^{M-1} x[i+j]$$

where x = the input signal, y = the output signal and M = the averaging factor.

2.3 Modular Display system

An electronic display system was used to display an unvarying visual environment in the flight arena. A fly was usually tethered and surrounded by the cylindrical flight arena. Earlier studies utilized a rotating mechanical cylinder to display the visual stimulus (Götz, 1968). This original apparatus has recently been improved by replacing the mechanical components with an electronic controller system (Reiser & Dickinson, 2008). This display system, combined with wing beat analyzer equipment, was used for the spontaneous flight behavior studies. A homogeneously illuminated electronic arena was used in this study. There was only nonpatterned, uniform green illumination on the arena wall.

Hardware setup

The electronic display system contained a circular array of light-emitting diodes (LED) panels (BM-10288MI, American Bright Optoelectronics Corp., Magnolia Ave, Chino, USA), two panel controller boards (PCB) and a Panel Display Controller (PDC) (Mettrix Technology Corp., Hopewell Junction, New York, USA). Each LED module (32 mm × 32 mm × 19 mm) consisted of an 8 X 8 matrix array of green LEDs with an attached microprocessor unit. The cylindrical arrays of LED

panels were assembled in 4 X 12 LED panel formations making up a volume of 1448 cm^3. This cylindrical unit was positioned between two panel controller boards (PCB). One of the PCBs was connected to the PDC (Fig. 4). In this specific setup, no coupling was established between the flight arena and the wing beat analyzer's left (L) and right (R) wing beat amplitudes, thereby leaving open the feedback loop between the fly's behavior and the panorama.

The angle between adjacent LEDs was 1.7°. The luminescence of the arena was 72 cd/md^2, and the contrast level at maximum display was 92%. Each LED was refreshed at 370 Hz (Reiser & Dickinson, 2008), which is below the flicker fusion rate of the fly (~200 Hz). The spectral intensity was ~0.4 at an intensity level of –3, and the wavelength of each LED was ~560 nm. This wavelength has been shown to drive R1-R6 photoreceptors in *Drosophila* (Wu & Pak, 1975). The room lights were turned off during the machine operation. Because this methodology of assembling the arena and programming the panels and control programs was adapted from a web resource https://bitbucket.org/mreiser/panels/wiki/Old_Panels_Info, no detailed steps to program individual LED panels and assemble the arena are provided in this section.

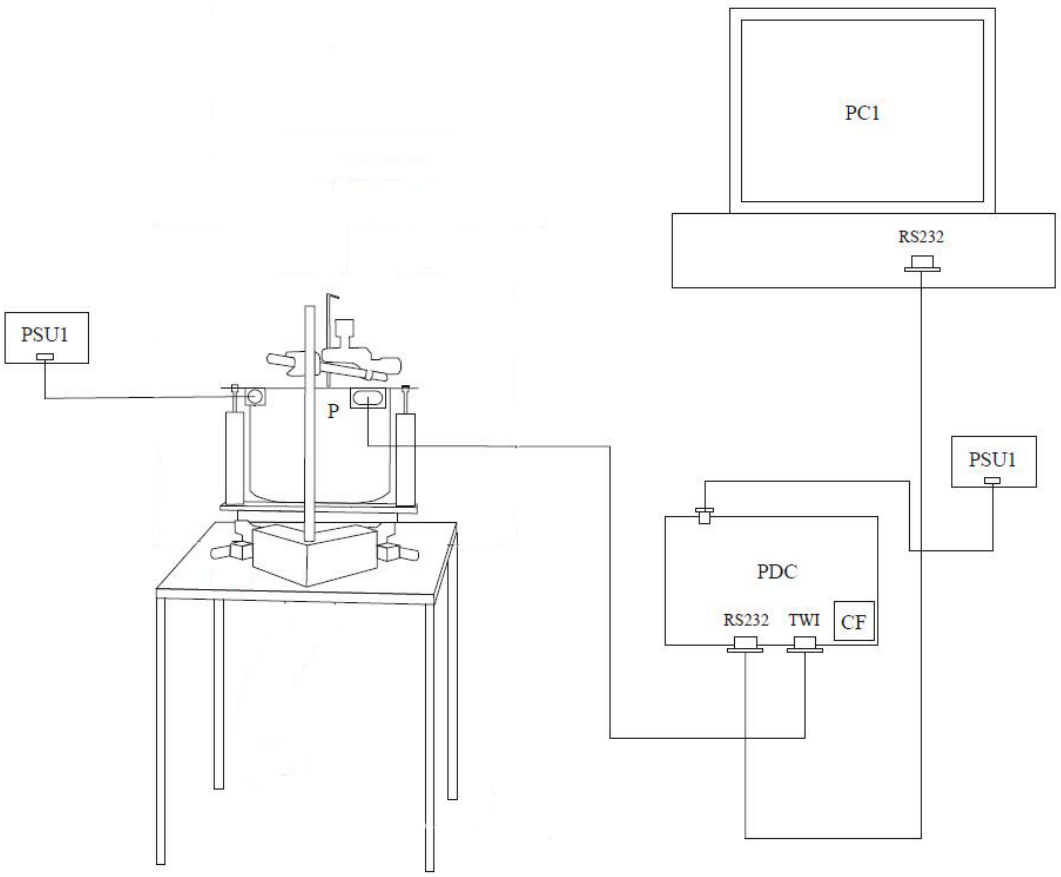

Fig. 4. Schematics of the LED arena setup.

An insect Panel Display Controller (PDC) retrieves display patterns from a memory card (CF) and transmits them to each panel (P) through a TWI connector. A control program in the computer (PC1) connected with the PDC via RS232 offers GUI-based controls to access the display parameters. All units are powered by a 5 V DC power supply unit (PSU1).

Overview of working components

PC software: We used a MATLAB-based software program for communication with the PDC. This program is accessible via the MATLAB software to generate patterns, control intensity and communicate with the controller boards. The intensity level was set to 3 units to maintain constant illumination.

Panel Display Controller (PDC): The panel display controller consists of a dual microcontroller circuit unit. A flash microcontroller unit (ATmega8, Atmel Corp., San Jose, CA, 95110, USA) reads pattern data from the CF card and delivers it to the main microcontroller unit. The main controller receives the data from the PC control program over the serial port (RS232) and maintains display updates. It also communicates with external devices over Analog Input (AI), Analog Output (AO), and Digital Input/output (DIO) ports.

Computer system (PC1): Intel Pentium 4 CPU 1.60GHz, 2 GB RAM, NVIDIA Quadro4 700 XGL, Maxtor 53073H6 75GB HDD, Windows 7.

An Atmel AVR ISP MKII in-system programmer (SKU: ATAVRISP2, Atmel Corporate Headquarters, 1600 Technology Drive, San Jose, CA 95110, USA.) was used to program the microcontroller units (MCUs) of the LED panels and the panel display controller (PDC). This flash programming was done using a soft kit Atmel AVR studio 4 software package (http://www.atmel.com/tools/avrstudio4.aspx).

A CompactFlash card (CF): Traveler CompactFlash, 64 MB, was used to store the pattern data.

Panel unit (P): The panels are individual display modules with an 8 X 8 green dot matrix array of LEDs and a supporting microcontroller unit (MCU) to refresh the display locally. An MCU receives the pattern data and refreshes the LED display in every LED panel.

2.4 Analysis of yaw torque data

2.4.1 Fast Fourier Transform (FFT)

Fast Fourier Transform (FFT) was used to detect the frequency components of any oscillations arising from the fly behavior or the equipment. The FFT function in MATLAB transforms the time domain of a discrete time series sequence into a frequency domain. MATLAB software functions

(http://www.mathworks.de/de/help/matlab/ref/fft.html) were used for these transformation. These functions utilize the following equation.

The functions Y = fft(x) and y = ifft(X) implement the transform, given for vectors of length N by

$$X(k) = \sum_{j=1}^{N} x(j)\omega_N^{(j-1)(k-1)}$$

$$x(j) = (1/N)\sum_{k=1}^{N} X(k)\omega_N^{-(j-1)(k-1)}$$

where

$$\omega_N = e^{(-2\pi i)/N}$$

is an Nth root of unity (Duhamel P, 1990).

The window length of the raw data was converted to a length (N) to increase the calculating efficiency for the relatively larger datasets.

2.4.2 S-Map procedure

The S-Map procedure was applied to the yaw torque signals obtained from the wing beat analyzer equipment. S-Map stands for a sequentially locally weighted global linear map. The S-Map procedure is a tool that can be used to quantify the nonlinearity of given time series data by utilizing nonlinear forecasting analysis. This tool is able to detect a pattern in data that otherwise appear to be random using sample prediction and the complexity of the dynamic system. The given dataset is broadly considered to arise from a dynamic system that is bound to dynamic rules. The dynamic system determines the unique successor stage at any consecutive time after sampling the first half of state variables. If the system is linear, the initial conditions can be used to determine the subsequent state of the linear system. When the system does not follow the linearity equation, the system tends to deviate from an ideal linearity. In that case, the system can be a nonlinear dynamic system.

The S-Map procedure takes the first half of the points in a time series and predicts the second half of the data series. The first half of the data points is embedded to create attractor values, which are then used to predict the second half of the time series. Embedding is basically plotting time values against past values of the data. The general idea is that past values can be used to reconstruct the equation that generated those values. The shape that emerges from this embedding is called an "attractor". The second half of a time series of values can be predicted using this equation. An algorithm selects points that have histories similar to the initial points and that fall near the predicted values of the attractor. A new regression is computed for every prediction such that the vectors that are most similar to the predicted values are weighted more heavily. The points near the predicted values have more influence on the shape and direction of a line. All (not just some) of the points chosen are projected, and those points are exponentially weighted (Maye et al., 2007). If the system is globally linear, the best forecasts use all of the points in the attractor and not under-represent any of them. The accuracy of these predictions is evaluated by the coefficient of correlation between the predicted and the observed series.

However, if the relationship between actual and predicted data is more complicated, then the models increase the weighting parameter (Φ) to access the nonlinear status of the system (higher correlation values when $\Phi > 0$). If the manifold is dominated by noise, it appears as being only weakly nonlinear. So the S-Map method offers more skillful forecasts.

The function w is used to weight the library vectors by their distance to the prediction vector:

$$w(\mathbf{v}_1,\mathbf{v}_2) = \exp\left(-\theta \frac{\|\mathbf{v}_1 - \mathbf{v}_2\|}{\bar{w}}\right), \bar{w} = \frac{1}{|\boldsymbol{L}|}\sum_{i=1}^{|\boldsymbol{L}|} \|\boldsymbol{l}_i - \boldsymbol{p}^t\|.$$

For $\Phi = 0$, a linear map is obtained. Increasing Φ puts increasingly greater emphasis on the library vectors close to the prediction vector. MATLAB scripts for

the S-Map analysis were obtained from Dr. Alexander Maye, University Medical Center Hamburg-Eppendorf, Germany.

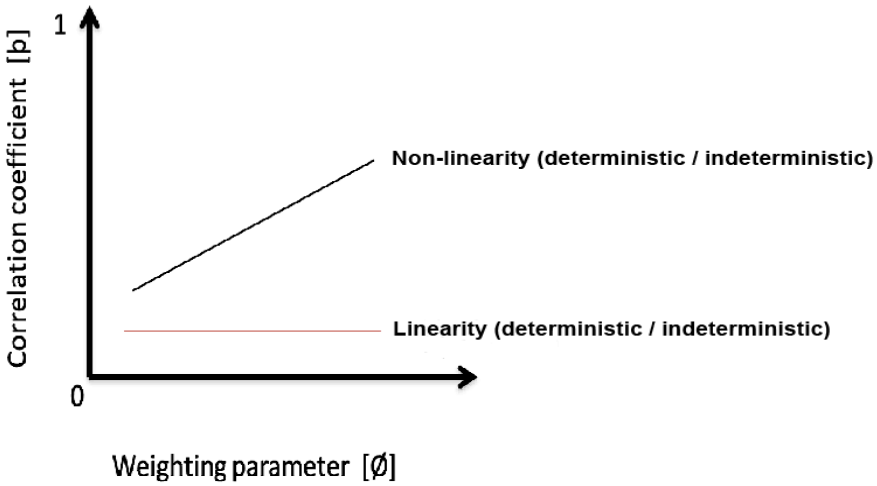

Fig. 5. A simplified interpretation of the S-Map analysis.

The correlation coefficient of the actual and predicted data against the weighting parameter is plotted. A shallow curve results if the relationship between the actual and predicted matrices is globally linear. When this relationship is complicated, weight is given to the predicted dataset to access the nonlinearity of the system (Maye et al., 2007). Thus, by increasing the weighting parameter, the steepness of the curve would indicate the presence of a nonlinear signature.

Quantification of the S-Map procedural results

The steepness of the curve over an increasingly weighted parameter in S-Map analysis determines the level of nonlinearity. A shallow curve indicates a globally linear signature in the S-Map procedure (Maye et al., 2007). Thus, the slope of a least-square regression line is calculated to estimate the nonlinearity of a time

series. A first-degree polynomial curve, in a least square sense in MATLAB software (function: 'polyfit'), was used to calculate the slope coefficients. The increase in the slope value denotes the estimated increase of a nonlinear signature.

2.4.3 Spike detection algorithm

Torque spikes were detected by applying spike detection algorithms. The spike detection algorithms written in the MATLAB software were adapted from Maye et al., 2007.

Raw yaw torque data were first filtered by a direct form II transposed implementation of the standard difference equation. Maximal and minimal values were detected from the filtered matrices by shifting the filtered values step-by-step in an array according to the user-defined threshold and step length. These maximum and minimum values were sorted out as spikes over the defined step length. The variables closest to a sorted variable were ignored using defined step lengths. Amplitude threshold levels were set from -1 to 1, depending on the filtered signal's amplitude. A detection frequency of 150 Hz was used.

2.4.4 Geometric Random Inner Product (GRIP) analysis

A GRIP analysis was implemented on the intervals between each torque spike. The GRIP procedure, developed by Maye et al., 2007, was used in this study to quantify the deviation from theoretically expected ideal randomness. Randomness is defined in terms of radioactive decay (Krane, 1988), whereas non-randomness was quantified by excess repetitions (i.e., repeats) or alternations between the successive bits (i.e., switches). The GRIP analysis assumes that a given vector represents a randomly distributed sequence. The average inner product of randomly distributed vectors in n-dimensional geometric objects is aggregated according to object-specific constants. The deviation from these constants was used as a measure of the randomness of a given dataset. This method is applied to the inter-saccade intervals (ISI) and inter-activity interval datasets with the Buridan paradigm to assess the randomness of the inter-event interval distribution.

2.5 The Buridan Paradigm

2.5.1 Flies

Experimental flies (mixed sex unless otherwise stated) 2-3 days old were anesthetized by briefly exposing them to carbon dioxide gas. One-third of a wing was left intact and rest was clipped using a pair of fine scissors. Wing-clipped flies were kept overnight in small containers with sugar granules and moistened tissue paper.

In brief, the Buridan paradigm (Colomb et al., 2012) device was used for automatic tracking of a walking fly given free choice between two visual landmarks in order to assess general locomotor competence. General characteristics of walking flies such as duration of walking, speed, etc. was calculated from this paradigm.

2.5.2 Hardware components

The Buridan paradigm consists of three components: a cylindrical arena, a standard USB camera (Logitech Quickcam Pro 9000) and a computer system.

The cylindrical unit consists of a round platform measuring 117mm in diameter. The cylinder was illuminated by four circular fluorescent tubes surrounding it (Osram, L 40w, 640C circular cool white).The four fluorescent tubes are located outside the cylindrical diffuser positioned at a distance of 147.5 mm from the center of the arena. Alternating current (1 kHz) was provided to the tubes by an electronic control gear (Osram Quicktronic QT-M 1×26–42). The inner area of the cylinder was outfitted with two opposing horizontal stripes inaccessible to the flies. The stripes were taped to the inside of the diffuser and each stripe measures 30mm X 313mm X 1mm. A standard USB camera was placed above the arena as depicted in Fig. 5 and the camera is connected to the computer running tracking programs. A wing-clipped fly was placed in a center of the platform during an experiment. The temperature on the platform during the experiment was 27°C, and

the luminosity ranged from 7.5 to 8 klx, with light intensity ranging from 370 to 850 nm.

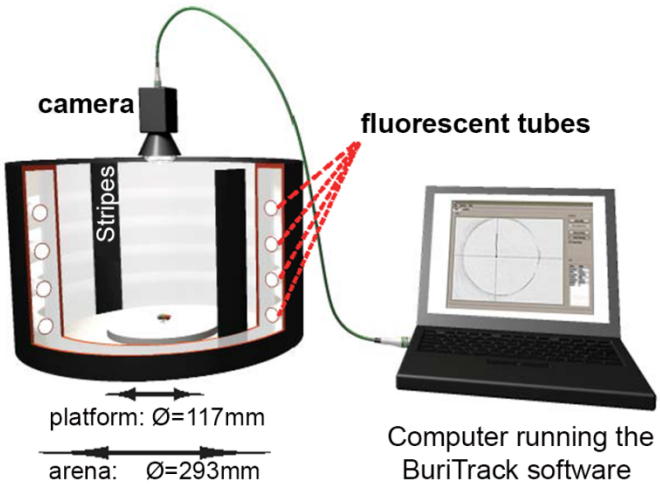

Fig. 6. Picture of the Buridan paradigm setup:

A wing-clipped fly was placed in the middle of a platform (117 mm diameter). The cylindrical arena surrounding the platform was constantly illuminated by fluorescent tubes. This arena was furnished with two horizontal black stripes measuring 30 mm wide, 313 mm high and 1 mm thick. A water canal between the arena and platform prevents the fly from reaching the stripes. The fly's position is captured on video using the standard USB webcam and transmitted to the tracking algorithm for extracting fly trajectory coordinates. (Cartoon Source Colomb et al., 2012).

2.5.3 Tracking software BuriTrack

An open source Buridan paradigm software package containing the tracking programs and analysis scripts were downloaded from http://buridan.sourceforge.net/ and installed on the computer. BuriTrack is a tracking program that captures the darkest spot in a given pixel range determined by a user threshold. This spot is taken as the assumed position of the fly. The tracking program stops and records a burst event whenever the fly jumps outside of the platform boundary. The final

trajectory data (X, Y in pixels), the time stamp and burst counts were saved as a text file (ASCII). The total duration of the experiment was set to 20 min. The graphical user interface offers the flexibility of choosing the threshold and other tracking factors.

2.5.4 CeTrAn Centroid Trajectories Analysis software

The dataset generated by a BuriTrack algorithm was analyzed using a CeTrAn trajectory analysis algorithm written in open source statistics package R (http://r-project.org/). The graphical user interface given in the package (Colomb et al., 2012) was utilized to import the trajectory dataset. The median speed, meander, and activity parameters were computed using the analysis program.

2.5.5 General activity measurement

Activity and median speed

The algorithm considers every movement an activity and every absence of movement longer than 1 s is taken as a pause (shorter periods of rest were considered active periods). Activity was calculated in seconds. Speed was calculated by dividing the distance over instant speed of each movement of a fly (mm/s). The mean of the median speed of each fly was calculated to measure the speed performance of the group. Speed value exceeding 50 mm/s was considered a jump and was not included in the calculation.

Computer-generated walking data

The computer-generated data was obtained from the following web source: http://buridan.sourceforge.net/. These data samples were generated by modifying the R code from an adehabitat package. The direction was set to follow a correlated walk. An initial angle was chosen randomly and the next one was generated following a wrapped normal distribution around the previous angle. The correlation strength between two consecutive turning angles was determined by a variable 'r'. A step length for the 8999 movements (900 seconds at 10 Hz) was created by multiplying a Boolean variable simulating pauses (1 or 0, randomly generated using a uniform distribution with adjustable frequency "f") with a speed value that was

created by drawing from a Chi distribution around a mean value "h" (correlated walk) (Colomb et al., 2012).

The position was calculated iteratively, starting at the center of the arena. When the position fell outside the boundary, it was replaced by the nearest point within the limits of the arena and the angle sequence was recalculated taking the first angle randomly. Accordingly, the next movement will lie outside of the platform with a probability >0.5.

2.5.6 Inter-activity interval extraction

Activity intervals were extracted from Buridan activity datasets. The time interval between each start of activity was considered an inter-activity interval. In Buridan's paradigm, every movement is considered an activity and every absence of movement longer than 1s is a pause (shorter periods of rest were considered active periods). These inter-activity intervals were tested for randomness using GRIP analysis.

2.6 pySolo assay

2.6.1 Flies

Experimental flies 2-3 days old were kept overnight in small fly containers with a few sugar granules and moistened paper. The next day, the flies were loaded into a pySolo chamber for experimentation.

pySolo is a python-based tracking program designed for drosophila sleep and locomotor pattern analysis (Gilestro, 2012). pySolo was used to measure the locomotor activity performance of the *Drosophila*. All tracker programs, analysis scripts and detailed instructions on setup and usage were obtained from a web resource www.pysolo.net.

2.6.2 Hardware components

The setup consists of 12 test tubes, each measuring 70mm X 3mm, a cardboard box, low voltage infrared light emitting (IR-LED) diode stripes (BLO106-15-29, Conrad electronics, Germany), a USB camera (Logitech Quickcam Pro 9000) and a computer.

Each tube was sealed with food on one side and a cotton stopper on the other. These tubes were placed together a few millimeters apart inside the box and closed with a transparent sheet. Infrared red light emitting diode stripes were placed above these tubes to illuminate the setup without any reflective glare. The camera was placed above this box, in such a way that the individual test tubes were visible in the pySolo video monitor. The IR filter was removed from the USB camera to capture the infrared illumination (Fig.7).

2.6.3 Configuration

pySolo tracking software was installed on the computer with an Ubuntu operating system (10.04.4 LTS-Lucid Lynx) as per the instructions given in the web tutorials from www.pysolo.net. Once installed on the computer, pySolo is accessed through the command line by typing the following command:

pysolo_anal.py -c alternative_options.opt

This will start a program along with an optional file for editing any user preferences. An intuitive graphical user interface offers the flexibility of editing preferences. The following parameters were set to record from a single camera monitoring system.

The essential data to be filled in are in the first window, under 'Files and Folder'. They are

- the DAM folder
- the output folder

- the extension of the input files
- the RAW data structure

The RAW data structure was set to record the virtual beam split functionality of the monitoring system. The output file format was set to .txt.

2.6.4 Midline crossing events

Before the experiments began, each individual fly was reared inside a tube using a mouth pipette. Infrared-illuminated flies appear brighter than the background image in a video. A tracking program uses a camera placed above the tubes to track the movement of the brightest spot. The resulting trajectory units for individual flies were stored as a multi-dimensional array of objects in a text file.

An activity event was recorded whenever a fly crossed the imaginary midline of a tube (Fig. 7 A). These counts were registered in the output text file. The bin width of sampling was 1 minute. The total duration of tracking was 24 hours, and daytime data were used for analysis.

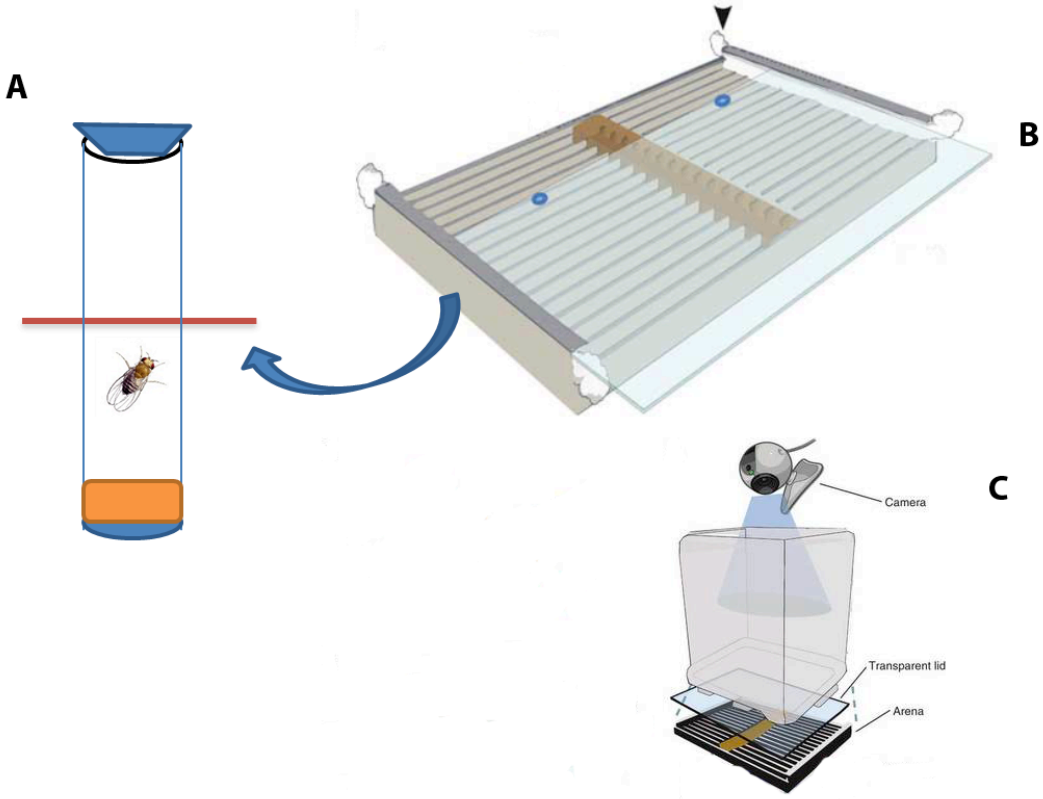

Fig. 7. (A) The pySolo experimental setup.

An individual fly was secured inside the test tube with access to fly food. The red line indicates the imaginary midline of the tube. (B). All tubes with flies were placed on a cardboard stage. (C) A USB camera was positioned above the fly tubes. The tracking program recorded each instance of a fly crossing the imaginary midline as a separate event for each fly. This entire setup was illuminated by an infrared light strip. (Image adapted from Gilestro, 2012).

2.7 Fly Siesta and Burstiness analysis

FlySiesta, a MATLAB based program, was used to analyze burstiness, i.e., long pauses with clustered activity, of the midline crossing activity event intervals from the pySolo assay. Various studies (Barabasi, 2005; Gilani & Hövel, 2012; Sorribes et al., 2011; Webb, 2002) have demonstrated that activity intervals

generated by biological systems follow certain statistical properties. The dynamics of many events offer quantitative understanding of complex mechanisms. For example, the Poisson process can be used to characterize physiological events. While each event is independent of any other event at any other time, i.e., the event has no "memory", a point Poisson process is often used to describe the events.

A Weibull distribution was applied to the entire inter-activity interval distribution to assess the burstiness parameter. The scale (λ) and shape (k) parameters of the Weibull distribution help determine the degree of burstiness. The scale parameter is linearly correlated with the mean Inter-activity intervals (IAIs), and the shape parameter is useful to parameterize the given distribution. A k-value of less than 1 denotes bursty behavior of the distribution, whereas a k of 0 corresponds to a Poisson distribution.

The pySolo midline crossing event datasets were transformed into activity bouts (ABs) using tState2eps.m. IAI's were calculated from midline crossing event vectors using the tstate2ievs.m function in the FlySiesta toolbox. The burstiness parameter was calculated using these bouts and intervals. All of these programs were downloaded from (https://github.com/dePolaviejaLab/FlySiesta/downloads) Ms. Amanda Sorribes, Universidad Autonoma de Madrid, Spain, who kindly provided the base programs.

2.8 Statistical analysis

Statistical analysis was performed using One-Way Analysis of Variance (ANOVA) in the MATLAB software for between-group comparisons. The Kolmogorov-Smirnov test was used to check the distribution of a given dataset. All error bars represent one standard error of the mean (s.e.m), and the p-value of a statistical test is represented by stars: one star ($p<0.05$), two stars ($p<0.01$), three stars ($p<0.001$).

3. RESULTS

3.1 No-noise frequency components from the wing beat analyzer

Highly accurate and precise measurement of the wing beat amplitudes of fruit flies in a wing-beat analyzer requires suppression of noisy signals from the equipment. This would guarantee that the obtained wing stroke amplitudes represent only the frequency components from the fly behavior and are not contaminated by the instrumentation. Wing-beat amplitude signals were first measured without using an actual WTB fly to identify any frequency noise components from the equipment. Wing stroke amplitudes were optimized by analog signal band pass filtering and moving average filtering of the yaw torque digital signals (see Methods, 2.2). MATLAB software functions were used to perform power spectral analyses to identify frequency components from the yaw torque signals before and after signal optimization. Before signal optimization, power spectral analysis (Fig. 8A) detected frequency components ranging from 4 – 11 Hz in the higher power range. After signal optimization, peak frequency components of the oscillations were effectively suppressed (Fig. 8B), and no visible frequency components appeared even in the lowest power range.

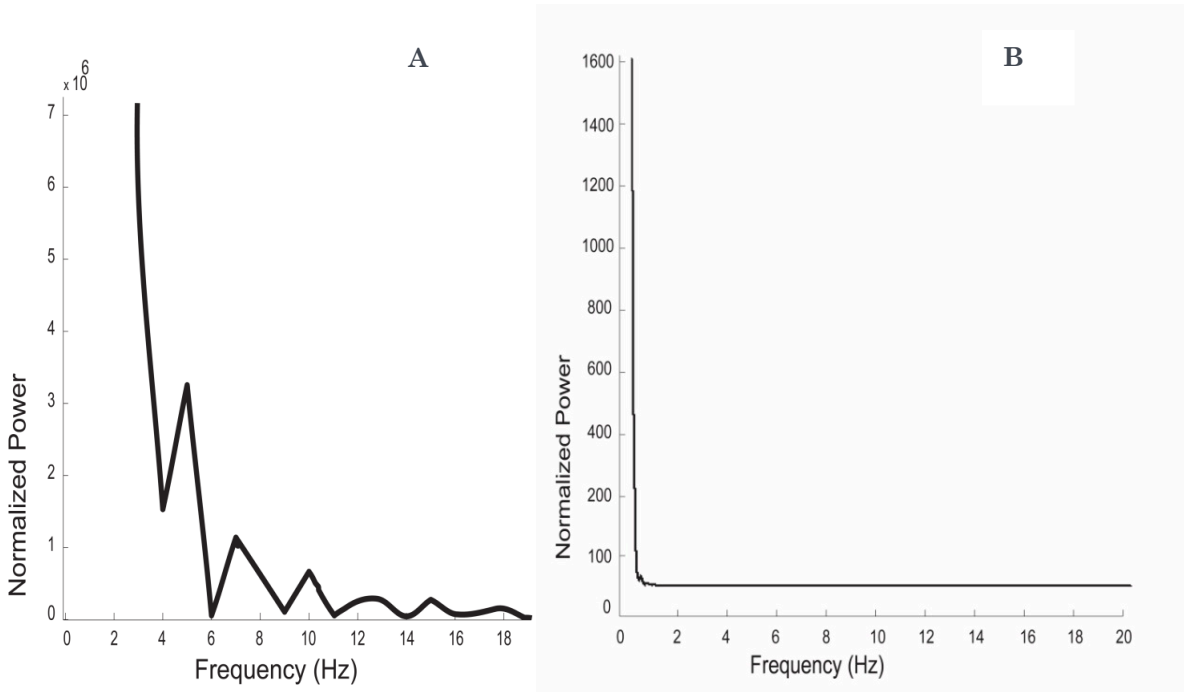

Fig. 8. Power spectral analysis on a yaw torque signal obtained from the wing beat analyzer.

This graph illustrates the average power spectral densities of the yaw turning signals obtained from the wing beat analyzer before (A) and after (B) signal optimization without using an actual fly. Average power spectra of 0 - 20 Hz calculated from 30 trials of open loop experiments; duration of each trial was 500 s. **A**. Frequency components of 4 – 11 Hz in the higher power range were identified. B. No peak frequency components were observed in the lower power ranges.

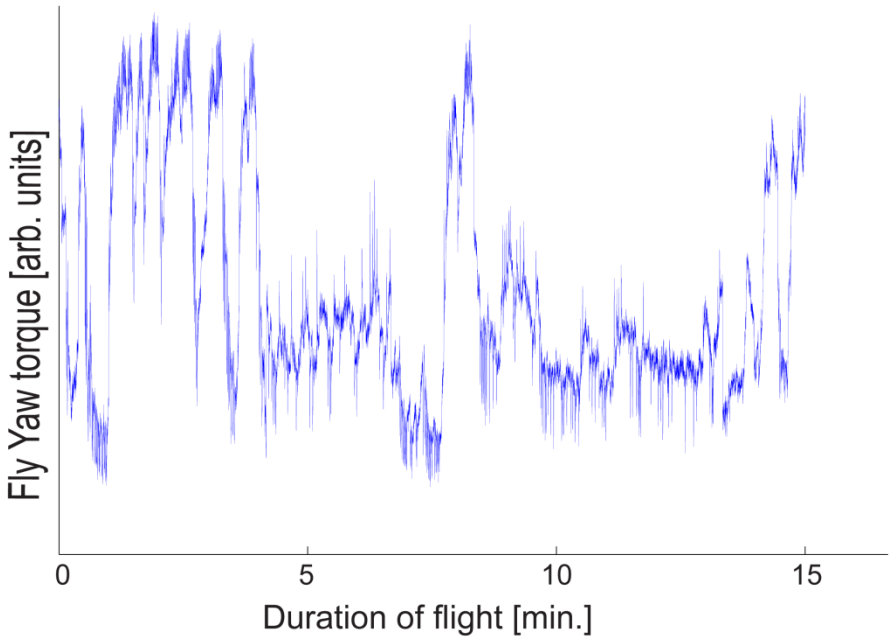

Fig. 9. A typical yaw torque signal.

Plotted is the typical yaw torque signal obtained from the wing beat analyzer equipment from a single WTB fly for 15 min. Yaw torque was calculated from the difference between the left and right wing beat amplitudes (L minus R).

3.2 S-Map analysis can be used with variable flight duration

Correlations between the duration of flight and S-Map procedural results were estimated to determine the minimum length of the yaw torque dataset required for the S-Map procedure. Transgenic flies were expected to have highly variable flight durations during the open loop control. This tool has been used on flight datasets with fixed flight durations of 30 min. over several trials. Therefore, it was necessary to evaluate the correlation between the time duration of flight behavior and the S-Map procedural results. The slope of the S-Map procedural results was taken to correlate with the duration of flight in minutes (Fig. 10). WTB flies that flew for various durations were used. In general, no correlation (Pearson's correlation coefficient r = 0.34) was observed between the duration of flight and the

S-Map nonlinearity curve in the wild type flies (WTB). However, the linear correlation was robust in the lower left quarter of the graph (below 6 min.), and the rest of the points (pink) were randomly distributed. Therefore, the yaw turning dataset values below 6 min. were excluded from the analysis described below.

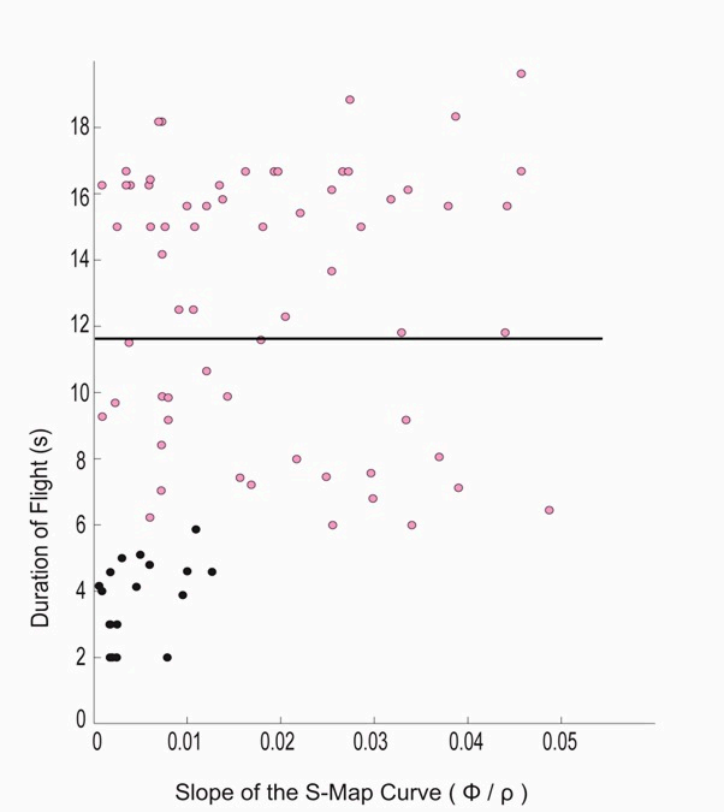

Fig. 10. The correlation between the flight durations of WTB flies and the slopes of the S-Map signature.

Plotted is the slope of the S-Map curve against the duration of flight (s). Black points indicate the cluster of slope values below 6 min. The rest (pink points) were the slopes of S-Map results above 6 min. (N=78). A Pearson product-moment correlation coefficient was calculated (r=0.34, $P < 0.001$) after removing the slope values below 6 min., and the corresponding linear fit is indicated by the black line

3.3 Screening for neuronal candidates that generate linear signatures in S-Map analysis

To identify specific groups of neuronal cells that might be responsible for spontaneous yaw torque behavior in *Drosophila*, offspring of several enhancer trap P [Gal4] lines, with an expression pattern in distinct regions of the central complex and mushroom body regions, crossed with UAS-TNT-E were screened for linearity. Yaw turning behavior was recorded from these transgenic flies and S-Map analysis was performed on the resulting flight datasets. The slope of the S-Map procedural results was taken as a measure of nonlinearity. Screenings were done on 9 P [Gal4] lines, with WTB flies serving as a control group. A majority of tetanus toxin-expressed fly lines produced an increasing nonlinear signature (Fig. 11). However, one fly line (double transgenic c232; c105-Gal4 X UAS-TNT-E) with silenced ellipsoid body ring neurons showed a linear signature. This was the only fly group that did not show nonlinearity in the screening process, indicating that the hypothesized neuronal circuitry for spontaneous nonlinear generation. Previous work by Neuser, Triphan, Mronz, Poeck, & Strauss, 2008 presented an expression pattern in ellipsoid body ring neurons R3-R4d and R1 in c232-Gal4 and c105-Gal4 fly lines, respectively. The fly line that showed nonlinearity consisted of these two transgenic c232-Gal4 & c105-Gal4 lines.

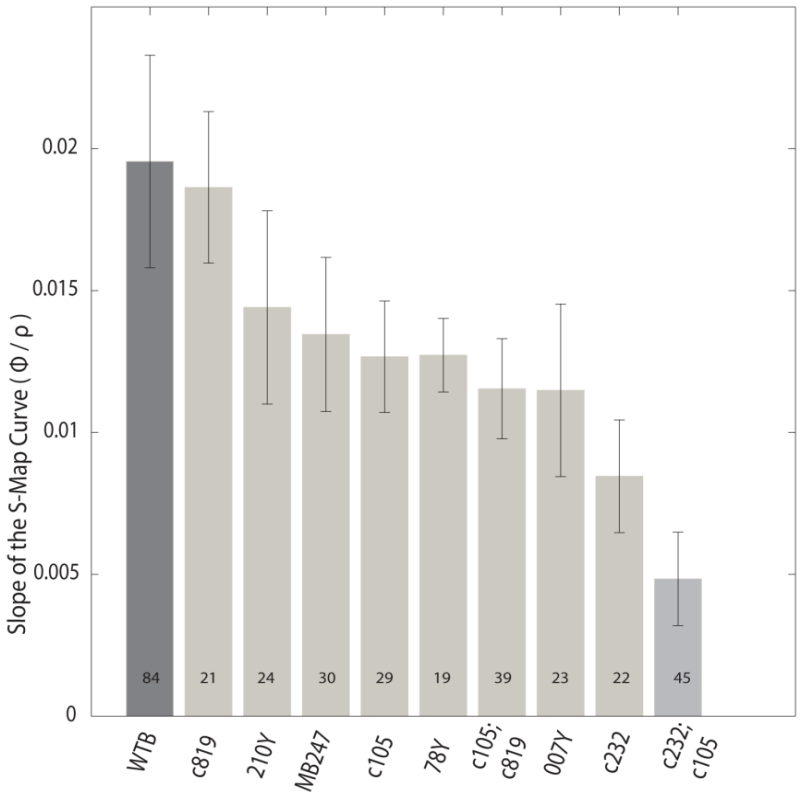

Fig. 11. Comparison of the average slopes of the nonlinearity curve obtained from the S-Map procedure from a variety of P [Gal4] lines expressed with tetanus toxin. Mushroom body lines (mb247-Gal4 and 210y-Gal4) showed improved nonlinearity skills along with the control group (WTB, dark grey). In addition to the 78y-Gal4, the c819-Gal4 line showed relatively better nonlinear signals. The double line C105; C819 Gal4 was not affected by the expression of tetanus toxin for nonlinear generation. However, double C232; C105 Gal4 flies displayed a linear signature (light grey). However, the c105-Gal4 and c232-Gal4 flies exhibited nonlinear prediction skills in the analysis. Error bars represent the mean ± s.e.m.

3.4 Linear structure in S-Map analysis from double c232; c105-Gal4 caused by tetanus toxin expression

Ellipsoid body ring neuronal cells R1, R3 and R4d were previously found to be a necessary component of a nonlinear signature in spontaneously generated yaw torque behavior. The double c232: c105-Gal4 X UAS-TNT-E fly line was tested

earlier, using WTB flies as a control group. Generally, transgenic fly lines tend to drift toward other genotyped fly lines over several generations (Belle & Heisenbergt, 1996). A double transgenic fly line that showed linear prediction skills was tested with its genetic control groups (c232; c105-Gal4 X WTB and WTB X TNT) to determine the influence of genetic background on the ability to generate a linear phenotype and to reveal any false positive results in the screening procedure. Measurements of yaw torque behavior of these three groups were taken simultaneously to nullify any effect of environmental variables. The genetic controls exhibited increased slope values, suggesting a nonlinear signature. In contrast, the tetanus toxin-expressed group (double c232; c105-Gal4 X UAS-TNT-E) showed a linear signature that was significantly different from that of the control group (Fig. 12, $p<0.001$). These results were similar to those of the screening experiments. Thus, the linear phenotype is produced by tetanus toxin expression, not by genetic background. This result in turn confirms the presence of neuronal cells that are a necessary component of nonlinear generation of spontaneous behavioral variability.

Fig. 12. Genetic ablations of R1, R3 and R4d ellipsoid body ring neurons abolish the nonlinear signature.

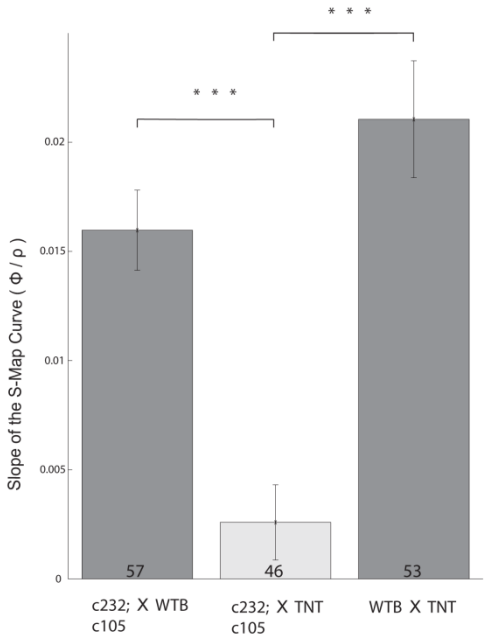

The double transgenic c232; c105-Gal4 X TNT generated linear signature in the S-Map procedure is indicated by lower slope values compared to nonlinear trend generation with increased slope values by control groups (c232; c105-Gal4 X WTB and WTB X TNT, dark grey). One-way ANOVA (***$p<0.001$).

Error bars represent the mean ± s.e.m.

3.5 Neuronal organization for nonlinearity generation

Individual transgenic fly lines of a double transgenic line were tested, and the S-Map procedure was implemented to narrow the search to specific parts of the identified candidate neuronal cells. The way in which an identified neuronal population is organized into functional ensembles to mediate nonlinear behavior is not known. Thus, we further dissected the identified neuronal substrate to investigate this organization.

Tetanus expression of the candidate neuronal cells in the ellipsoid body was driven by the combination of two transgenic fly lines, i.e., c232-Gal4 and c105-Gal4. The linear phenotype was exhibited in this double transgenic fly line. The double transgenic line, when separated, yields two individual transgenic fly lines, c232-Gal4 and c105-Gal4, each with a reduced expression pattern on a specific pool of neuronal cells.

The offspring of individual lines (c232-Gal4 and c105-Gal4) crossed with UAS-TNT-E were tested for nonlinear generation. Both lines generated yaw torque signals with increased nonlinear prediction skills. In both cases, there was no significant difference between them and their respective genetic control group (Fig. 13, $P > 0.05$).

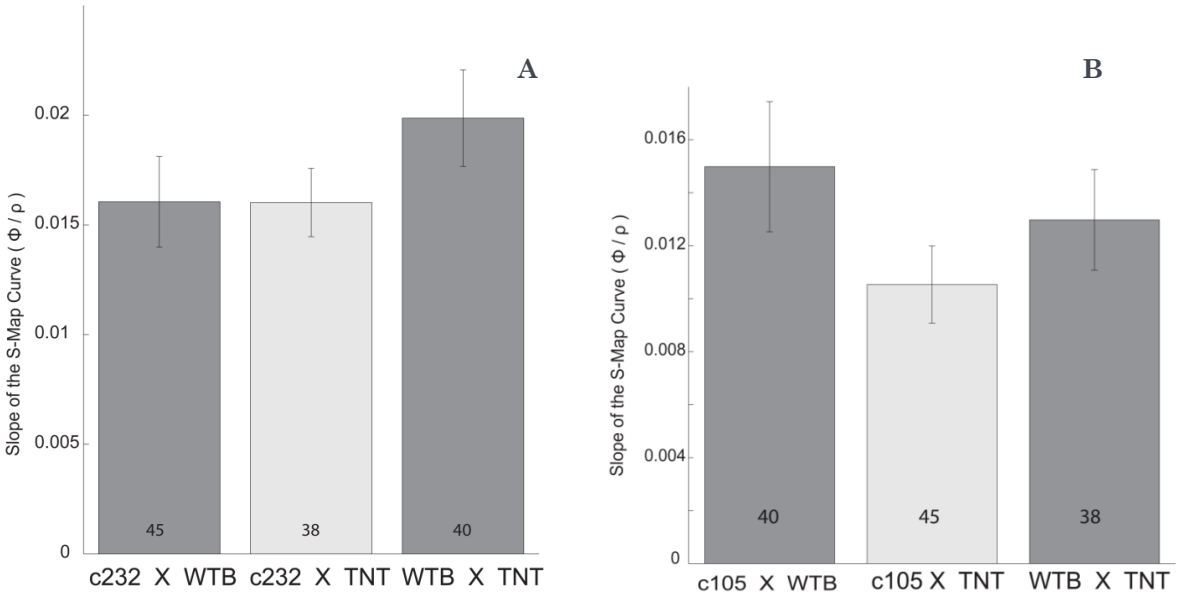

Fig. 13. There is no change in nonlinearity generation when any of the ellipsoid body ring neurons (R3, R4d or R1) is silenced alone.

Plotted (A and B) are the average slope values from the S-Map analysis of the tetanus-expressed c105-Gal4 and c232-Gal4, and their genetic controls (dark grey). The c232 X TNT, c105 X TNT lines and their respective genetic controls showed a nonlinear signature. Error bars represent the mean ± s.e.m.

3.6 Locomotor competence of candidate fly line

We measured the general locomotor competence of the double c232; c105-Gal4 X TNT fly line to determine whether the ellipsoid body ring neurons (R1, R3 and R4d), whose mediation generates a nonlinear signature, were involved in controlling locomotor behavior. This fly line was chosen as an ideal candidate for further characterization.

Although the linear signature provided evidence that certain neurons were mediating the nonlinear signature in spontaneous behavioral variability, causality could not be established without characterizing the role of these neurons in other associated behaviors. The perturbation of specific ellipsoid body ring neurons might result in loss in the nonlinear phenotype of associated locomotor behaviors. The linear phenotype could possibly have arisen due to a defect in locomotor activity. For this reason, we assessed the yaw torque generation functionality and walking activities of the candidate fly line. We also quantified the inter-torque spike interval distribution of yaw torque and the inter-activity interval distribution of walking. The activity assays also made it possible to scrutinize the correlation between the linear phenotype and any defect in locomotion. The data (Figs. 14, 15 and 16) suggested that torque spike generation, walking activity and walking speed were unaffected in the candidate fly lines. The results from these studies strengthened our finding of the specific role of identified neuronal circuits in nonlinear generation.

3.6.1 Measurement of yaw torque spikes

Yaw torque spikes were calculated as a measure for yaw torque generation functionality. During tethered flight, flies generate abrupt, short bursts of turns with changing turn orientation (Fig. 9). Automated algorithms of spike sorting were used to count the spikes from raw yaw torque data. The results indicate that the frequency of spike generation (~1 Hz) by the candidate fly lines was not different (Fig. 14, $p>0.05$) from that of the control groups. Candidate fly lines were able to generate torque spikes during tethered flight conditions under a uniform visual environment.

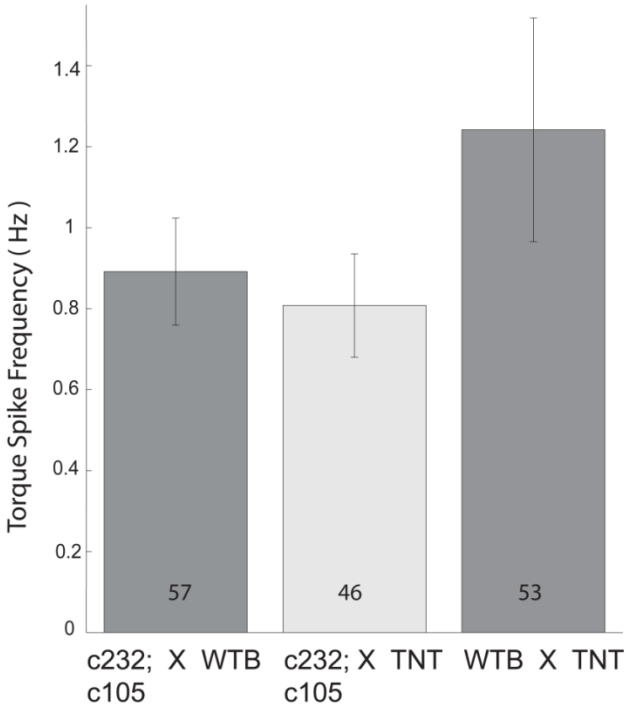

Fig. 14. Candidate fly lines were able to generate unaffected torque spikes.

Plotted bars are the frequency (Hz) of torque spikes generated by double c232; c105-Gal4 X TNT and its genetic controls c232; c105 X WTB & WTB X TNT (dark grey). Error bars represent the mean ± s.e.m.

3.6.2 Walking Activity measurement

We performed a Buridan paradigm activity assay with wing-clipped flies to evaluate the walking activity of the candidate fly lines. Walking activity period and speed were calculated from the trajectories of the flies steadily walking back and forth when black stripes were presented as visual cues. Each trial lasted for 20 min., and the candidate fly lines and their respective genetic control groups were tested in parallel. Total walking activity time of c232; c105 X TNT was statistically distinguishable (Fig. 15, $p<0.01$) from one genetic control group c232; c105 X WTB. However, another control group, WTB X TNT, showed walking activity that was indistinguishable from that of the tetanus-expressed group. However, no severe walking activity deficiency was identified in the tetanus toxin-expressed fly group. Additionally, the mean of the median walking speeds of all of the groups (Fig. 16) ranged from 16-18 mm/s, and candidate fly groups were able to generate normal walking speeds.

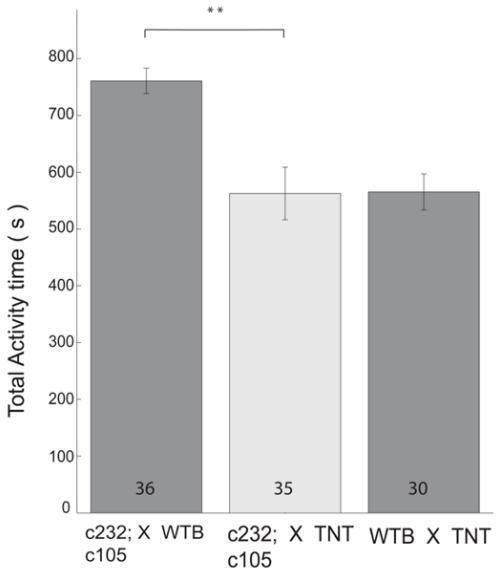

Fig. 15. No deficit in time course of walking activity.

Plotted are the mean total activity times (s) by candidate fly line double c232; c105-Gal4 expressed with tetanus toxin and its genetic control (dark grey) groups (c232; c105-Gal4 X WTB & WTB X TNT). Statistics were performed as a One-Way ANOVA (**$p<0.01$). Error bars represent the mean ± s.e.m.

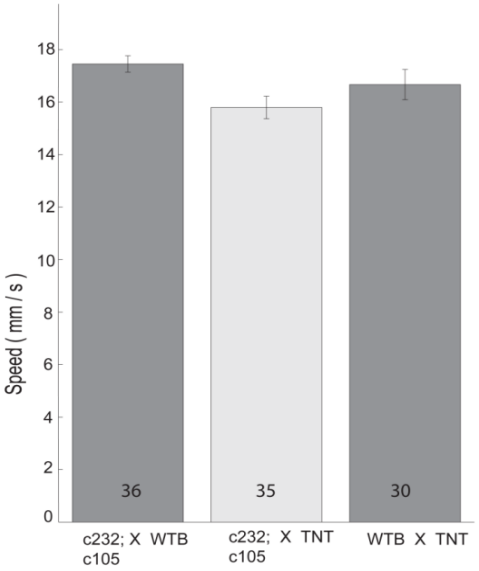

Fig. 16. Mean walking speed in transition between two landmarks in the Buridan Paradigm.

Plotted are the means of the median speed of candidate fly line c232; c105-Gal4 X TNT and its two genetic control (dark grey) groups. Bars represent the mean ± s.e.m.

3.6.3 Inter-event interval distribution analysis

Previous results have shown that the yaw torque spikes in overall locomotor activity, such as the duration of walking and walking speed, display the characteristics of functional locomotor apparatus. A quantitative analysis of the inter-event intervals was performed using GRIP analysis and burstiness parameter analysis to determine whether a specific group of neurons, i.e., ellipsoid body ring neurons (R1, R3 and R4d), was also involved in maintaining the temporal pattern of locomotor activity in *Drosophila*. The inter-torque spike intervals and inter-walking activity intervals from the Buridan paradigm were chosen for the GRIP analysis. Flies from the line c232; c105 Gal4, with tetanus expression in ellipsoid body ring neurons R1, R3 and R4d, deviated from perfect randomness (SD = 0 is random) in their inter-torque spike interval distribution (Fig. 17) and inter-walking activity distribution (Fig. 18). The standard deviations of randomness in both measures in genetic controls also indicated that their walking intervals were distributed nonrandomly. Inter-walking activity intervals were obtained by subtracting the time (s) between each start of walking activity in the Buridan paradigm.

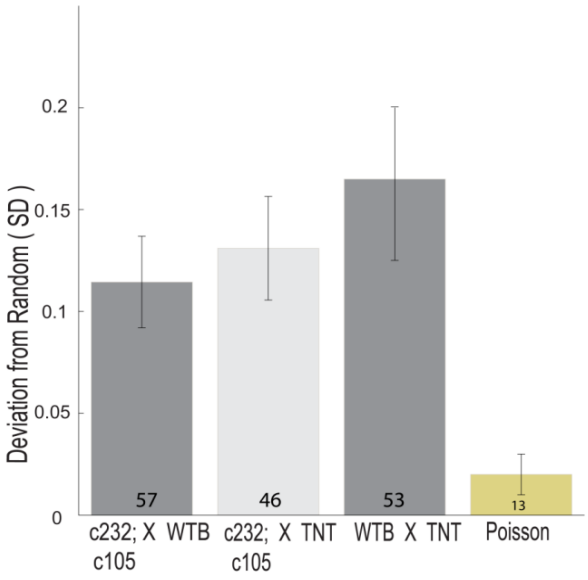

Fig. 17. GRIP analysis on inter-torque spike intervals (ISIs).

Plotted are the mean standard deviations of a theoretically predicted random value for the fly ISI series and the Poisson process. C232; c105 Gal4 X TNT and its respective genetic control groups (dark grey) deviated from the Poisson process (yellow), which remained close to random values. A standard deviation (SD) value of 0 would indicate perfect randomness. Bars represent the mean ± s.e.m.

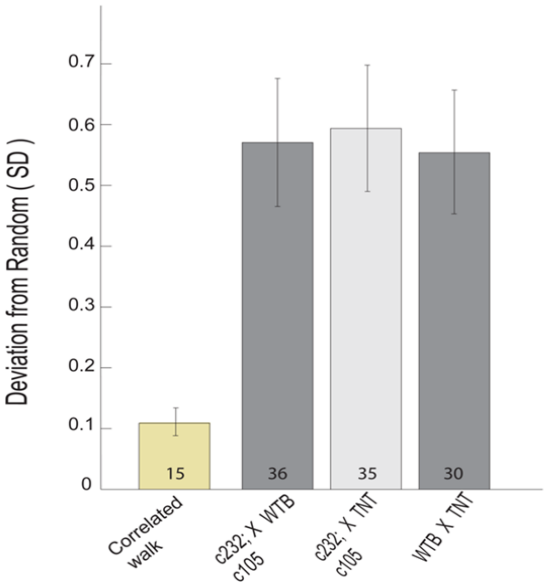

Fig. 18. Inter-walking activity intervals were non-random: GRIP analyses on time intervals.

Bars represent the mean standard deviations from a perfect randomness value calculated from the intervals between each start of walking activity from double c232; c105-Gal4 expressed with tetanus toxin, and its genetic control (dark grey) groups (c232; c105-Gal4 X WTB and WTB X TNT). GRIP analysis results on inter-activity intervals extracted

from computer-generated walking (correlated walk) are plotted in dark grey. Bars represent the mean ± s.e.m.

Burstiness parameter

The candidate neuronal circuits were further tested for their role in burstiness generation. Midline crossing activity from the pySolo experiments was used to generate inter-activity intervals on which to perform behavioral burstiness analysis. The expression of tetanus toxin in the ellipsoid body ring neurons had no involvement in generating behavioral burstiness in the candidate line or its genetic control. These results (Fig. 19) were consistent with the finding that impairment of the central complex function does not affect burstiness (Sorribes et al., 2011).

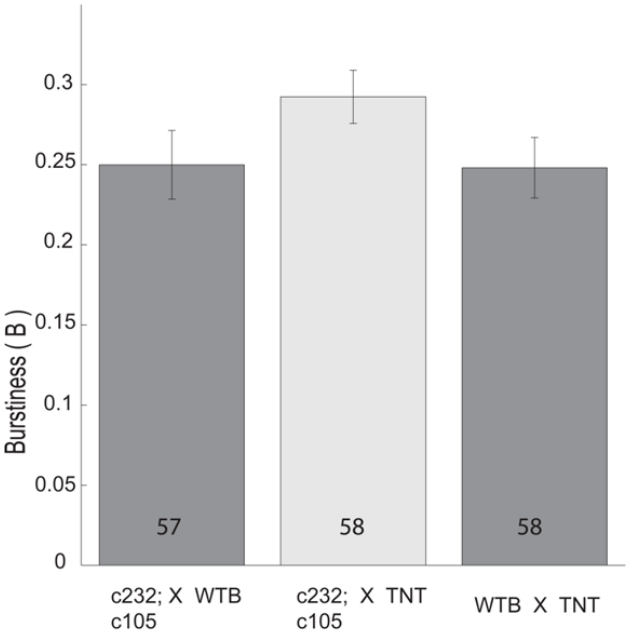

Fig. 19. Impairment in ellipsoid body ring neurons does not affect burstiness.

Plotted is the burstiness parameter (B) generated by the Double Gal4 c232; c105 X TNT line and its genetic controls (dark grey). All three groups generated bursty activity as indicated by a burstiness parameter value B>0 that was well above the Poisson process. Error bars represent the mean ± s.e.m.

4. DISCUSSION

The neuronal basis of spontaneous behavior was explored in this study using a combination of interdisciplinary approaches. *Drosophila* offered a unique and advantageous model system for studying the neural basis of spontaneous yaw turning behavior. This study probed the neuronal cells contributing to variability in spontaneous yaw turning behavior in *Drosophila*, using genetic dissection and mathematical tools such as the S-Map procedure and GRIP analysis. This approach proved to be effective in identifying the part of neural circuits that facilitates a nonlinear temporal structure in spontaneous flight behavior and in identifying the neuronal architecture of the circuits. The temporal properties of spontaneous yaw turning behavioral variability were shown to be mediated by a group of cells (R1, R3 and R4d) in the ellipsoid body neurons of *Drosophila*. The identified neuronal cells were further characterized for their role in associated locomotor behavior. This characterization, using walking activity assays, supported the specific role of the identified neural cells in nonlinearity generation. The temporal pattern of locomotor activity was also measured to discover its role in fine regulation of locomotor activity.

4.1 Neural circuitry underlying spontaneous behavioral variability

4.1.1 Ellipsoid body ring neurons mediate the nonlinear structure in spontaneous flight behavior

Our initial screening showed that spontaneous actions generated by fruit flies are possibly mediated by specific neuronal regions (Fig. 11). Among eight different fly lines, only those with silenced ellipsoid-body ring neurons R1, R3 and R4d did not show nonlinear structure in the S-Map procedure. The fly lines with a silenced mushroom body did exhibit an increased nonlinear signature. Thus mushroom body integration is not required for nonlinear configuration in spontaneous behavior. Additionally, fly lines in which other substructures of the central complex (the

proto-cerebral bridge, the fan-shaped body and noduli) were silenced did confirm a nonlinear prediction. To summarize, the genetic ablation of specific ring neurons in the ellipsoid body region alters the temporal structure of spontaneous yaw torque behavior toward a more linear signature. These results might suggest the presence of designated circuits for mediating spontaneous variability. The screening procedure was able to identify the neuronal components that were responsible for a nonlinear structure in spontaneous flight behavior.

Linear structure was confirmed by testing the candidate fly lines and their appropriate genetic control groups (double c232; c105-Gal4 X WTB and WTB X UAS-TNT). Linear structure could have been influenced by a false positive genotype factor and by other environmental conditions that prevailed during the screening procedure. However, the test results indicated that the changes in nonlinearity were caused by the expression of tetanus toxin on the R1, R3 and R4d region of the ellipsoid body and were not influenced by any other variables. Initial studies of the behavioral variability indicated the presence of intrinsic brain components that could act as a deterministic system to generate nonlinear spontaneous variability (Maye et al., 2007). In our study, we most likely isolated only that part of the neuronal circuitry that mediates temporal properties of spontaneous behavior in fruit flies.

4.1.2 The temporal pattern of spontaneous behavioral variability and its independence from associated locomotor activity

Tetanus toxin (TeTxLC) expression, especially on central complex sub-structures, has been shown to cause severe locomotor defects (Martin et al., 2002; Martin, Raabe, & Heisenberg, 1999; Strauss, 2002; Martin & Robinow, 2003). In our study, the candidate line had an expression pattern in the ellipsoid body ring neurons R1, R3 and R4d, which are part of the central body substructure. Still unanswered is the question of whether the circuits for nonlinear structure generation are part of the circuits maintaining general locomotor behavior.

Our results showed that candidate flies were endogenously generating stereotyped, short bursts of yaw torque in a uniform visual surrounding. The flies appeared to be able to generate normal short bursts of yaw torque, and the temporal characteristics of yaw turning had a linear signature in the S-Map analysis. This result generates the interesting hypothesis that the neural components involving yaw torque can be divided into two components: stereotyped yaw torque spike generators and a turning orientation initiator. One component circuit presumably generates the stable bursts of yaw torques independently of the other neural components, which initiate left- or right-turn orientation in a uniform visual environment. Support for this hypothesis also comes from the results of the inter-torque spike interval distribution analysis. The time intervals between subsequent torque spikes are distributed nonrandomly, following non-Poisson statistics, indicating that the ring neuronal cells might have an influence over the turning initiators.

Additionally, the time course of walking activity and walking speed showed no abnormalities. The reported walking speed of the WTB flies is from 11-18 mm/s (Neuser et al., 2008; Strauss et al., 1992). We showed here that the walking speed was nearly the same in the candidate fly line. Subsequently, the interval between each start of walking activity was distributed nonrandomly, deviating from computer generated random values. The burstiness parameter, i.e., bursts of activity followed by long periods of inactivity, also describes a nonrandom phenomenon (Kerster & Schaeffer, 2013; Sorribes et al., 2011). The candidate line with silenced ellipsoid body ring neurons exhibits bursty dynamics that are significantly different from Poisson processes in the flies' midline-crossing walking activity. The temporal dynamics of walking activity thus appear to be normal. These results indicate that there are specific neural components that mediate nonlinear behavior but are not involved in generating locomotor behavior. A nonlinearity component in spontaneous behavior is thus generated robustly by the intrinsic brain structures of *Drosophila*.

This finding raises another question. If the fine regulation of spontaneous yaw torque behavior generates a nonlinear structure in the temporal pattern that is mediated by the ellipsoid body ring neurons and if the flies are able to initiate intact locomotor functionality as indicated by normal torque spikes and walking activities, then how could fine temporal pattern generation be organized with flight architecture? One probable answer is that the nonlinear circuits that depend on reduced sensory stimulus-response coupling may interact with the hard-wired circuit that generates stereotypic behaviors. Blocking a small number of neural cells in the central complex disturbs one particular property of the temporal pattern of endogenous flight behavior while associated flight behavior remains functional. Earlier studies reported that the substructures of the central complex are involved in the temporal pattern of walking activity (Strauss, 2002). Blocking the neurons that arborize the ellipsoid body affects the power law distribution of the spontaneous walking time interval (J Martin & Ernst, 2001a). However, these defects in temporal properties were shown to be independent of the fly's locomotor activity level. An earlier study suggested two possibilities regarding the relationship between normal walking activity and the temporal properties of walking (Martin & Ernst, 2001b). A general activity defect might be accompanied by disruption in temporal dynamics, or a defect in temporal dynamics coexists with normal behavioral activity. Our findings suggest the latter: a central complex substructure is responsible for the fine regulation of temporal pattern in flight behavior without affecting active flight generation.

However, any leaky expression of tetanus into, for example, other neurons or muscles during an animal's development could have profound detrimental effects on its normal development, which in turn could influence spontaneous behavior. The measures of the general flight and walking activity of our flies indicated no apparent defect in their locomotor physiology. It might have been helpful to take further behavioral readouts during the flies' development to better understand the role of candidate neural circuits in facilitating spontaneous behavioral variability.

For instance, the UAS-*shi* tool could have been used to temporarily manipulate synaptic activity.

4.2 Functional neuronal architecture for nonlinear structure generation

Because a specific group of cells in the fly brain functions as a neuronal substructure for regulating spontaneous variability, we further dissected parts of this circuitry. The double transgenic Gal4 line that showed linear structure consisted of two individual lines, c105 Gal4 and c232 Gal4. The ring neuron R1 and R3-R4d of the ellipsoid body region are silenced by tetanus toxin expression in individual fly lines c105-Gal4 and c232-Gal4 (Neuser et al., 2008). The yaw torque characteristics of these individual lines showed increasingly nonlinear solutions in the S-Map analysis. While nonlinearity was abolished when silencing the combination of ring neurons, selectively silencing an individual (R1) ring neuron or a combination of ring neurons (R3 and R4d) did not have any effect on nonlinearity. This result reveals an organized neural entity for mediating nonlinear structure in spontaneous behavioral variability. When either of the ring neurons (R1 or R3 and R4d) was severed, the other could possibly have been supplemented by another surrounding neuronal population to form a local network that served as a functional entity to generate nonlinear functionality in fly behavior. In any event, ellipsoid body ring neurons are essential components of the neuronal circuitry mediating variability in flight behavior.

Earlier flight control studies (Ilius, 2007) examined mutant alleles of the gene *ellipsoid body open* (*ebo*) of *Drosophila*. The central complex substructures of the *ebo* mutants show such defects as a divided fan- shaped body, a ventrally open, flattened and occasionally divided cleavage in the ellipsoid body and a proto-cerebral bridge with bead-like appearances. These mutant flies execute normal motion-induced torque modulations but their spontaneous torque amplitudes are reduced compared to wild type flies. These defects in the central complex substructure were associated with spontaneous flight behavior. The *ebo* mutations broadly affected the ellipsoid body, fan-shaped body and mushroom body calyx

structures. This wide range of structural defects (Strauss et al., 1992) could affect several locomotor parameters. Though these *ebo* mutation studies initiated behavioral studies of spontaneous flight, they did not include in-depth examination of the neural entities and their underlying functional structures. We were able to identify the group of ring neuronal cells that are responsible for the temporal characteristics of spontaneous flight behavior.

4.3 Level of brain organization: Connecting endogenous flight behavior with intrinsic brain organization

The nonlinear temporal structure generated during behavioral variability is controlled by ellipsoid body ring neurons. This finding, as well as that of Maye et al., 2007, demonstrates that deterministic components control behavioral variability. We showed that the interruption of a specific neural circuit obstructed nonlinearity in temporal yaw torque behavior. This shift toward linear dynamics has implications for understanding neural circuit functionality.

The spontaneous actions generated by flies are highly variable. We have shown in this study that variable behavioral components have a particular temporal structure and are modulated by neuronal components. The behavioral variability is controlled by neuronal components instead of occurring randomly. Conversely, flies orient toward stripes while fixating on objects by reducing their variability in turning attempts (Dickinson 2005; Götz 1968; Götz 1987). Behavioral variability has to be reduced to execute a specific task. It would be interesting to know how a fly switches between spontaneous actions and a stereotyped, stimulus-induced response such as stripe fixation in tethered flight.

Default mode network (DMN) activity in humans, which has been shown to be the primary cause of behavioral variability, is negatively correlated with task-induced brain activity (Fox & Raichle, 2007; Raichle, 2010). Spontaneous neuronal activity in the default mode network is suppressed during the task, and task-induced brain networks become active. The comparison of spontaneous variability

in insects with higher order biological systems is useful because the arthropod central complex brain region and vertebrate basal ganglia are homologous. The complex modulatory circuits of the ellipsoid body in arthropods share organizational features with the pallidum of vertebrate basal ganglia. The pallidum of ganglia plays an important role in action-selection among behavioral modules and their corresponding adaptive behaviors (Reiter & Bier, 2002; Strausfeld & Hirth, 2013). These similarities suggest the value of a direct comparison of the organization of the default mode network and the spontaneous behavior architecture supported by ellipsoid body regions. If spontaneous behavioral properties across these two biological systems are indeed homologous, the switch from spontaneous neural activity to task-specific activity could occur in the fly brain as well (e.g., as in stripe fixation). Independent functional connectivity studies on fly neuronal networks are required to shed light on endogenous brain organization.

This present study suggests that intrinsic properties of the ellipsoid body neurons facilitate temporal variability in yaw torque behavior in an environment that is known to cause no yaw turns. Thus, a simple "sensory-input-triggering-motor-output (yaw torque)" analogy (Censi et al., 2013) is not sufficient to explain the spontaneous actions generated by tethered flies. The finding of neuronal cells being responsible for spontaneous behavior could open up an avenue to apply intrinsic output-input transformations to an understanding of flight control mechanisms.

4.4 Future outlook: Do nonlinear circuits control operant activity initiation?

It has been proposed that operant learning requires the active initiation of behavior rather than simply responding to stimuli (Maye et al., 2007; Wolf & Heisenberg, 1991). According to this proposal, the sensory cues present in the flight simulator do not necessarily initiate the yaw turns. The temporal correlation between the presence of complex stimuli and motor commands may merely indicate a motivation for learning. In our study, flies initiated yaw turns voluntarily in an

environment known to cause no yaw turns. During spontaneous behavior, an ecologically relevant search strategy (Wolf & Heisenberg, 1984) might engage the motor commands to initiate yaw saccade turns to learn the consequences of actions. The present study has postulated the involvement of neural circuits in the fine maintenance of yaw torque turning in a uniform visual environment. If the identified neural circuits were indeed necessary for spontaneous actions, the next phase of study would be to access the candidate fly's ability to actively initiate actions and learn the consequences of the actions during the presence of aversive cues. Such a study could impose a new characterization of the candidate neural circuits that has relevance to operant activity and operant conditioning. The ideal paradigm to access the learning strategy would be to use the closed loop flight torque meter with no visual cues.

Flies would be placed in a flight simulator with a uniform visual environment, and subjected to aversive stimuli e.g., laser heat shock, that would be applied while the fly was attempting to turn to one side (either left or right). If the flies were able to comprehend the negative consequences of the actions, as indicated by avoiding the punished left or right side, operant modulation could be silencing the candidate neuronal cells. Alternatively, the candidate neural circuits might have a profound effect on the operant conditioning. This perspective could provide insight into understanding the neuronal mechanisms for action-selection and self-learning.

5. SUMMARY:

Neuronal cells interact to produce a diverse behavioral organization. Cooperation among designated neuronal populations of several cells leads to endogenous behavioral generation that is not driven by stimuli. This property distinguishes the brain from an automated, stimulus-driven artificial entity. These spontaneous behaviors represent intrinsic properties of the specific neuronal circuits. The primary aim of this study was to identify the neuronal components underlying the mediation of spontaneous yaw torque behavior in *Drosophila*. The role of various neuronal populations in spontaneous behavior generation was investigated using genetic dissection and mathematical tools, such as the S-Map procedure and GRIP analysis. A screening procedure was implemented on a group of Gal4 fly lines with an expression pattern in various cells of central complex structures and mushroom bodies in the fly brain to identify the candidate neurons. Locomotor assays were performed using Buridan and pySolo paradigm to complement the role of candidate neuronal circuitry on associated locomotor behavior. The present studies were performed using *Drosophila melanogaster*, whose flight was studied using an optical wing beat analyzer. This insect offers an advantageous and powerful model system for a study such as ours that requires genetic accessibility and quantifiable flight behaviors.

Our screening procedure indicated that groups of ellipsoid body ring neuronal cells (R1, R3 and R4d) were associated with the temporal structure of spontaneous flight behavior. The nonlinear temporal structure observed in wild type flies shifted toward a linear signature in the S-Map procedure. The candidate fly line with silenced ellipsoid body ring neurons (R1, R3 and R4d) was tested with comparable genetic controls to rule out any false positive, genetic or other environmental influence over the shift in temporal structure in the screening procedure. This test confirmed the role of the ellipsoid body ring neurons R1, R3 and R4d in the temporal structure of spontaneous yaw turning behavior of fruit flies. Finally, these

neuronal populations appeared to have no influence over associated locomotor activities such as walking. To summarize, this study demonstrated the neuronal basis of spontaneous flight behaviors in *Drosophila* and may lead to future studies of intrinsic properties of the brain.

ZUSAMMENFASSUNG:

Neuronale Zellen interagieren um unterschiedliche Verhaltenweisen hervorzurufen. Die Zusammenarbeit von bestimmten Neuronenpopulationen führt zu Generierung von endogenem Verhalten das nicht durch Stimuli ausgelöst wird. Diese Eigenschaft unterscheidet das Gehirn von einer automatischen, Stimulus kontrollierten, künstlichen Funktionseinheit. Dieses spontane Verhalten ist eine intrinsische Eigenschaft von spezifischen neuronalen Schaltkreisen. Das Hauptanliegen dieser Studie war neuronale Komponenten zu identifizieren, die das spontane Gierungs-Drehmoment Verhalten in *Drosophila* vermitteln. Die Rolle von verschiedenen Neuronenpopulationen bei der Generierung von spontanem Verhalten wurde mit Hilfe von transgenen Fliegenlinien und mathematischen Methoden wie S-Map Verfahren und GRIP Analysen untersucht. Gal4 Fliegenlinien mit Expressionsmustern in unterschiedlichen Neuronen des Zentralkomplexes und der Pilzkörper wurden analysiert um Kandidatenneurone zu finden. Fortbewegungsanalysen wurden mit Hilfe von Buridan and pySolo Paradigmen durchgeführt um identifizierten Kandidatenneurone zu charakterisieren. Die vorliegende Studie wurde mit *Drosophila* melanogaster durchgeführt, deren Flug mit Hilfe eines optischen Flügelschlaganalysators untersucht wurde. *Drosophila* ist das beste Modellsystem um die neuronalen Grundlagen von spontanem Verhalten zu antdecken aufgrund der einfachen genetischen Manipulation und des quantifizierbaren Flugverhaltens.

Unsere Untersuchungen deuten darauf hin, dass eine Gruppe von Ringneuronen im Ellipsoid-Körper (R1, R3 und R4d) mit dem zeitlichen Aufbau von

spontanem Flugverhalten assoziiert ist. Die nichtlineare zeitliche Struktur, die in Wildtypfliegen beobachtet wird, verändert sich zu einer linearen in der S-Map Analyse. Die Kandidatenfliegenlinie wurde mit vergleichbaren genetischen Kontrollen getestet um auszuschließen, dass genetische und andere Umwelteinflüsse die Veränderung der zeitlichen Struktur verursacht haben. Dieser Test bestätigt die Rolle der Ringneurone des Ellipsoid-Körper R1, R3 und R4d bei dem Gier-Moment-Verhalten der Fruchtfliegen. Zusätzlich scheinen diese Neuronen die Laufaktivität nicht zu beeinflussen. Zusammenfassend zeigt diese Studie die neuronale Grundlage von spontanem Flugverhalten in Drosophila und legt die Basis für weiterführende Studien an intrinsischen Eigenschaften des Gehirns.

6. BIBLIOGRAPHY:

Abarbanel, H. D., & Rabinovich, M. I. (2001). Neurodynamics: nonlinear dynamics and neurobiology. *Current opinion in neurobiology*, *11*(4), 423–30. Retrieved from http://www.ncbi.nlm.nih.gov/pubmed/11502387

Barabasi, A. (2005). The origin of bursts and heavy tails in human dynamics. *Nature*, *435*(May). doi:10.1038/nature03526.1.

Belle, J. S. D. E., & Heisenbergt, M. (1996). Expression of Drosophila mushroom body mutations in alternative genetic backgrounds : A case study of the mushroom body miniature gene (mbm), *93*(September), 9875–9880.

Berni, J., Pulver, S. R., Griffith, L. C., & Bate, M. (2012). Autonomous Circuitry for Substrate Exploration in Freely Moving Drosophila Larvae. *Current biology : CB*, 1–10. doi:10.1016/j.cub.2012.07.048

Borst, a, & Egelhaaf, M. (1989). Principles of visual motion detection. *Trends in neurosciences*, *12*(8), 297–306. Retrieved from http://www.ncbi.nlm.nih.gov/pubmed/2475948

Borst, a, & Haag, J. (2002). Neural networks in the cockpit of the fly. *Journal of comparative physiology. A, Neuroethology, sensory, neural, and behavioral physiology*, *188*(6), 419–37. doi:10.1007/s00359-002-0316-8

Borst, A. (2009). Drosophila's view on insect vision. *Current biology : CB*, *19*(1), R36–47. doi:10.1016/j.cub.2008.11.001

Borst, A., & Bahde, S. (1988). Visual information processing in the fly's landing system. *Journal of Comparative Physiology A*, *163*(2), 167–173. doi:10.1007/BF00612426

Borst, A., Haag, J., & Reiff, D. F. (2010). Fly motion vision. *Annual review of neuroscience*, *33*, 49–70. doi:10.1146/annurev-neuro-060909-153155

Brand, a H., & Perrimon, N. (1993). Targeted gene expression as a means of altering cell fates and generating dominant phenotypes. *Development (Cambridge, England)*, *118*(2), 401–15. Retrieved from http://www.ncbi.nlm.nih.gov/pubmed/8223268

Brembs, B. (2002). An analysis of associative learning in Drosophila at the flight simulator. Retrieved from http://www.opus-bayern.de/uni-

wuerzburg/volltexte/2002/103/

Buckner, R. L., Andrews-Hanna, J. R., & Schacter, D. L. (2008). The brain's default network: anatomy, function, and relevance to disease. *Annals of the New York Academy of Sciences*, *1124*, 1–38. doi:10.1196/annals.1440.011

Burke, R. E. (2007). Sir Charles Sherrington's the integrative action of the nervous system: a centenary appreciation. *Brain : a journal of neurology*, *130*(Pt 4), 887–94. doi:10.1093/brain/awm022

Card, G., & Dickinson, M. H. (2008). Visually mediated motor planning in the escape response of Drosophila. *Current biology : CB*, *18*(17), 1300–7. doi:10.1016/j.cub.2008.07.094

Censi, A., Straw, A. D., Sayaman, R. W., Murray, R. M., & Dickinson, M. H. (2013). Discriminating External and Internal Causes for Heading Changes in Freely Flying Drosophila. (O. Sporns, Ed.)*PLoS Computational Biology*, *9*(2), e1002891. doi:10.1371/journal.pcbi.1002891

Chow, D. M., Theobald, J. C., & Frye, M. a. (2011). An olfactory circuit increases the fidelity of visual behavior. *The Journal of neuroscience : the official journal of the Society for Neuroscience*, *31*(42), 15035–47. doi:10.1523/JNEUROSCI.1736-11.2011

Churchland, M. M., Yu, B. M., Cunningham, J. P., Sugrue, L. P., Cohen, M. R., Corrado, G. S., Newsome, W. T., et al. (2010). Stimulus onset quenches neural variability: a widespread cortical phenomenon. *Nature neuroscience*, *13*(3), 369–78. doi:10.1038/nn.2501

Collett, T. S. (2002). Insect vision: controlling actions through optic flow. *Current biology : CB*, *12*(18), R615–7. Retrieved from http://www.ncbi.nlm.nih.gov/pubmed/12372265

Colomb, J., Reiter, L., Blaszkiewicz, J., Wessnitzer, J., & Brembs, B. (2012). Open source tracking and analysis of adult Drosophila locomotion in Buridan's paradigm with and without visual targets. *PloS one*, *7*(8), e42247. doi:10.1371/journal.pone.0042247

Comer, C. M., & Robertson, R. M. (2001). Identified nerve cells and insect behavior. *Progress in neurobiology*, *63*(4), 409–39. Retrieved from http://www.ncbi.nlm.nih.gov/pubmed/11163685

Conner, W. E., & Corcoran, A. J. (2012). Sound strategies: the 65-million-year-old

battle between bats and insects. *Annual review of entomology*, *57*, 21–39. doi:10.1146/annurev-ento-121510-133537

D Roeder. (1964). The detection and evasion of bats by moths. *Smithsonian Annual report*.

Dewell, R. B., & Gabbiani, F. (2012). Escape behavior: linking neural computation to action. *Current biology : CB*, *22*(5), R152–3. doi:10.1016/j.cub.2012.01.034

Dickinson, M. (1993). The active control of wing rotation by Drosophila. *Journal of experimental …*, *189*, 173–189. Retrieved from http://jeb.biologists.org/content/182/1/173.short

Dickinson, M. H. (2005). The initiation and control of rapid flight maneuvers in fruit flies. *Integrative and comparative biology*, *45*(2), 274–81. doi:10.1093/icb/45.2.274

Domenici, P., Blagburn, J. M., & Bacon, J. P. (2011). Animal escapology II: escape trajectory case studies. *The Journal of experimental biology*, *214*(Pt 15), 2474–94. doi:10.1242/jeb.053801

Duffy, J. B. (2002). GAL4 system in Drosophila: a fly geneticist's Swiss army knife. *Genesis (New York, N.Y. : 2000)*, *34*(1-2), 1–15. doi:10.1002/gene.10150

Duhamel P. (1990). Fats Fourier Transforms: A tutorial review and a state of the Art. *Signal Processing*, *19*, 259–299.

Estes, W. (1965). A technique for assessing variability of perceptual span. *Proceedings of the National Academy of Sciences of …*, *0*(C), 403–407. Retrieved from http://www.ncbi.nlm.nih.gov/pmc/articles/PMC219678/

Faisal, a A., Selen, L. P. J., & Wolpert, D. M. (2008). Noise in the nervous system. *Nature reviews. Neuroscience*, *9*(4), 292–303. doi:10.1038/nrn2258

Farrow, K., Borst, A., & Haag, J. (2005). Sharing receptive fields with your neighbors: tuning the vertical system cells to wide field motion. *The Journal of neuroscience : the official journal of the Society for Neuroscience*, *25*(15), 3985–93. doi:10.1523/

Fox, M. D., Snyder, A. Z., Vincent, J. L., & Raichle, M. E. (2007). Intrinsic fluctuations within cortical systems account for intertrial variability in human behavior. *Neuron*, *56*(1), 171–84. doi:10.1016/j.neuron.2007.08.023

Frye, M. a, & Dickinson, M. H. (2004). Closing the loop between neurobiology and flight behavior in Drosophila. *Current opinion in neurobiology*, *14*(6), 729–36. doi:10.1016/j.conb.2004.10.004

Gilani, T., & Hövel, P. (2012). Dynamical Systems in Neuroscience. *Computational Neuroscience*. Retrieved from http://www.itp.tu-berlin.de/fileadmin/a3233_bccn-nachwuchsgruppe/dynamical_systems.pdf

Gilestro, G. F. (2012). Video tracking and analysis of sleep in Drosophila melanogaster. *Nature protocols*, *7*(5), 995–1007. doi:10.1038/nprot.2012.041

Götz, K. (1987). Course-control, metabolism and wing interference during ultralong tethered flight in Drosophila melanogaster. *Journal of experimental biology*, *46*, 35–46. Retrieved from http://jeb.biologists.org/content/128/1/35.short

Götz, K. G. (1968). Flight control in Drosophila by visual perception of motion. *Kybernetik*, *4*(6), 199–208. Retrieved from http://www.ncbi.nlm.nih.gov/pubmed/5731498

Griffith, L. C. (2012). Identifying behavioral circuits in Drosophila melanogaster: moving targets in a flying insect. *Current opinion in neurobiology*, *22*(4), 609–14. doi:10.1016/j.conb.2012.01.002

He, B. J., Zempel, J. M., Snyder, A. Z., & Raichle, M. E. (2010). The temporal structures and functional significance of scale-free brain activity. *Neuron*, *66*(3), 353–69. doi:10.1016/j.neuron.2010.04.020

Horridge, A. (2009). *What does the honeybee see?* The Australian National University E-Press.

Huston, S. J., & Jayaraman, V. (2011). Studying sensorimotor integration in insects. *Current opinion in neurobiology*, *21*(4), 527–34. doi:10.1016/j.conb.2011.05.030

Huston, S. J., & Krapp, H. G. (2009). Nonlinear integration of visual and haltere inputs in fly neck motor neurons. *The Journal of neuroscience : the official journal of the Society for Neuroscience*, *29*(42), 13097–105. doi:10.1523/JNEUROSCI.2915-09.2009

Ilius, R. W. and M. H. (2007). The central complex of Drosophila Melanogaster is involved in flight control: Studies on mutants and mosaics of the gene ellipsoid body open. *Journal of neurogenetics*, *21*, 321–338.

Janardan, K. G., Kerster, H. W., & Schaeffer, D. J. (2013). Biological Applications Poisson Distribution, *29*(10), 599–602.

Jenett, A., Rubin, G. M., Ngo, T.-T. B., Shepherd, D., Murphy, C., Dionne, H., Pfeiffer, B. D., (2012). A GAL4-driver line resource for Drosophila neurobiology. *Cell reports*, *2*(4), 991–1001. doi:10.1016/j.celrep.2012.09.011

Jimenez-Sanchez, C. (2012). Chemical effectors cause different motile behavior and deposition of bacteria in porous media. … *science & technology*. Retrieved from http://pubs.acs.org/doi/abs/10.1021/es300642n

Jung, S. N., Borst, A., & Haag, J. (2011). Flight activity alters velocity tuning of fly motion-sensitive neurons. *The Journal of neuroscience : the official journal of the Society for Neuroscience*, *31*(25), 9231–7. doi:10.1523/

Krane, K. S. (1988). Introductory Nuclear Physics. *John Wiley & Sons Inc,*.

Levine, D. N. (2007). Sherrington's "The Integrative action of the nervous system": a centennial appraisal. *Journal of the neurological sciences*, *253*(1-2), 1–6. doi:10.1016/j.jns.2006.12.002

Liu, G., Seiler, H., Wen, A., Zars, T., Ito, K., Wolf, R., Heisenberg, M., (2006). Distinct memory traces for two visual features in the Drosophila brain. *Nature*, *439*(7076), 551–6. doi:10.1038/nature04381

Louâpre, P., Van Alphen, J. J. M., & Pierre, J.-S. (2010). Humans and insects decide in similar ways. *PloS one*, *5*(12), e14251. doi:10.1371/journal.pone.0014251

M. R. A. Chance. (1957). The role of convulsions in behavior. *Systems research and behavioral science*, *2*(1), 30–45.

Maimon, G., Straw, A. D., & Dickinson, M. H. (2010). Active flight increases the gain of visual motion processing in Drosophila. *Nature Neuroscience*, *13*(3), 393–399. Retrieved from http://www.ncbi.nlm.nih.gov/pubmed/20154683

Mamiya, A., Straw, A. D., Tómasson, E., & Dickinson, M. H. (2011). Active and passive antennal movements during visually guided steering in flying Drosophila. *The Journal of neuroscience : the official journal of the Society for Neuroscience*, *31*(18), 6900–14. doi:10.1523/

Martin, J, Faure, P., & Ernst, R. (2001a). The power law distribution for walking-time intervals correlates with the ellipsoid-body in Drosophila. *Journal of neurogenetics*, *15*(3-4), 205–19. Retrieved from

http://www.ncbi.nlm.nih.gov/pubmed/12092904

Martin, J, Faure, P., & Ernst, R. (2001b). The power law distribution for walking-time intervals correlates with the ellipsoid-body in Drosophila. *Journal of neurogenetics*, *15*(3-4), 205–19. Retrieved from http://www.ncbi.nlm.nih.gov/pubmed/12092904

Martin, J.-R., Raabe, T., & Heisenberg, M. (1999). Central complex substructures are required for the maintenance of locomotor activity in Drosophila melanogaster. *Journal of Comparative Physiology A: Sensory, Neural, and Behavioral Physiology*, *185*(3), 277–288. doi:10.1007/s003590050387

Martin, JR, Keller, A., & Sweeney, S. (2002). Targeted expression of tetanus toxin: a new tool to study the neurobiology of behavior. *Advances in genetics*, *47*. Retrieved from http://www.sciencedirect.com/science/article/pii/S0065266002470010

May, M. (2012). Aerial Defense Tactics of Flying Insects some night-flying insects Preyed upon by echolocating bats , have developed acrobatic countermeasures to evade capture, *79*(4), 316–328.

Maye, A., Hsieh, C.-H., Sugihara, G., & Brembs, B. (2007). Order in spontaneous behavior. *PloS one*, *2*(5), e443. doi:10.1371/journal.pone.0000443

Miller, G. (1997). 12 Protean primates: The evolution of adaptive unpredictability in competition and courtship. *Machiavellian intelligence II: Extensions*

Milnik, A., Nowak, I., & Müller, N. G. (2013). Attention-dependent modulation of neural activity in primary sensorimotor cortex. *Brain and Behavior*, *3*(2), 54–66. doi:10.1002/brb3.114

Murray, M., & Wallace, M. (2012). *The Neural Bases of Multisensory Processes*. Frontiers in Neuroscience.

Nachtigall, W., & Wilson, D. M. (1967). Neuro-muscular control of dipteran flight. *The Journal of experimental biology*, *47*(1), 77–97. Retrieved from http://www.ncbi.nlm.nih.gov/pubmed/6058982

Nepomnyashchikh, V. a. (2013). Increases in variations in animal behavior induced by autocorrelations. *Biology Bulletin Reviews*, *3*(1), 49–56. doi:10.1134/S2079086413010064

Nepomnyashchikh, V. a., & Podgornyj, K. a. (2003). Emergence of Adaptive Searching Rules from the Dynamics of a Simple Nonlinear System. *Adaptive Behavior*, *11*(4), 245–265. doi:10.1177/1059712303114002

Nepomnyashchikh, V., & Podgornyj, K. (2003). A simple nonlinear dynamics may result in adaptive behaviors. *wsni2003.narod.ru*, 1–18. Retrieved from http://wsni2003.narod.ru/Papers/Nepomn2.pdf

Neuser, K., Triphan, T., Mronz, M., Poeck, B., & Strauss, R. (2008). Analysis of a spatial orientation memory in Drosophila. *Nature*, *453*(7199), 1244–7. doi:10.1038/nature07003

Oullier, O., Marin, L., & Stoffregen, T. (2006). Variability in postural coordination dynamics *system variability*. Retrieved from http://oullier.free.fr/files/2006_Oullier-Marin-Stoffregen-Bootsma-Bardy_Movement-System-Variability_Postural-Coordination-Dynamics.pdf

Proekt, A., Banavar, J. R., Maritan, A., & Pfaff, D. W. (2012). Scale invariance in the dynamics of spontaneous behavior. *Proceedings of the National Academy of Sciences of the United States of America*, *109*(26), 10564–9. doi:10.1073/pnas.1206894109

Raichle, M. E. (2010). Two views of brain function. *Trends in cognitive sciences*, *14*(4), 180–90. doi:10.1016/j.tics.2010.01.008

Reiser, M. B., & Dickinson, M. H. (2008). A modular display system for insect behavioral neuroscience. *Journal of Neuroscience Methods*, *167*(2), 127–139. doi:10.1016/j.jneumeth.2007.07.019

Reiter, L. T., & Bier, E. (2002). Using Drosophila melanogaster to uncover human disease gene function and potential drug target proteins. *Expert opinion on therapeutic targets*, *6*(3), 387–99. doi:10.1517/14728222.6.3.387

Renn, S. C. P., Armstrong, J. D., Yang, M., Wang, Z., An, X., Kaiser, K., & Taghert, P. H. (1999). Genetic Analysis of the Drosophila Ellipsoid Body Neuropil : Organization and Development of the Central Complex.

Roeder, K. (1962). The behaviour of free flying moths in the presence of artificial ultrasonic pulses. *Animal Behaviour*. Retrieved from http://www.sciencedirect.com/science/article/pii/0003347262900532

Saint-germain, A. M., Drapeau, P., & Buddle, C. M. (2009). Landing Patterns of Phloem- and Wood-feeding Coleoptera on Black Spruce of Different

Physiological and Decay States Landing Patterns of Phloem- and Wood-feeding Coleoptera on Black Spruce of Different Physiological and Decay States, *38*(3), 797–802.

Schmitt, F. G., & Seuront, L. (2001). Multifractal random walk in copepod behavior. *Physica A: Statistical Mechanics and its Applications*, *301*(1-4), 375–396. doi:10.1016/S0378-4371(01)00429-0

Sciences, B., & April, O. R. (1970). Protean Defence by Prey Animals, *302*, 285–302.

Series, S. A., & Note, A. (2000). Understanding Dynamic Signal Analysis. *Fundamentals of Signal Analysis Series*. Agilent Technologies.

Sherman, a. (2003). A comparison of visual and haltere-mediated equilibrium reflexes in the fruit fly Drosophila melanogaster. *Journal of Experimental Biology*, *206*(2), 295–302. doi:10.1242/jeb.00075

Sherrington, Charles Scott, Sir, 1857-1952. (1920). The integrative action of the nervous system. *New Haven Yale University Press*.

Sorribes, A., Armendariz, B. G., Lopez-Pigozzi, D., Murga, C., & De Polavieja, G. G. (2011). The origin of behavioral bursts in decision-making circuitry. *PLoS computational biology*, *7*(6), e1002075. doi:10.1371/journal.pcbi.1002075

Stein, R. B., Gossen, E. R., & Jones, K. E. (2005). Neuronal variability: noise or part of the signal? *Nature reviews. Neuroscience*, *6*(5), 389–97. doi:10.1038/nrn1668

Strausfeld, N. J., & Hirth, F. (2013). Deep Homology of Arthropod Central Complex and Vertebrate Basal Ganglia. *Science*, *340*(6129), 157–161. doi:10.1126/science.1231828

Strauss, R. (2002). The central complex and the genetic dissection of locomotor behaviour. *Current Opinion in Neurobiology*, *12*(6), 633–638. doi:10.1016/S0959-4388(02)00385-9

Strauss, R., Hanesch, U., Kinkelin, M., Wolf, R., & Heisenberg, M. (1992). Portrait of a structural brain mutant of the central complex, *8*, 125–155.

Sugihara, G., & Mayf, R. (1990). Nonlinear forecasting as a way of distinguishing chaos from measurement error in time series. Retrieved from http://books.google.com/books

Suster, M. L., Martin, J.-R., Sung, C., & Robinow, S. (2003). Targeted expression of

tetanus toxin reveals sets of neurons involved in larval locomotion in Drosophila. *Journal of neurobiology*, *55*(2), 233–46. doi:10.1002/neu.10202

Sweeney, S. T., Broadie, K., Keane, J., Niemann, H., & O'Kane, C. J. (1995). Targeted expression of tetanus toxin light chain in Drosophila specifically eliminates synaptic transmission and causes behavioral defects. *Neuron*, *14*(2), 341–51. Retrieved from http://www.ncbi.nlm.nih.gov/pubmed/7857643

Tammero, L. F., & Dickinson, M. H. (2002). Collision-avoidance and landing responses are mediated by separate pathways in the fruit fly, Drosophila melanogaster. *The Journal of experimental biology*, *205*(Pt 18), 2785–98. Retrieved from http://www.ncbi.nlm.nih.gov/pubmed/12177144

Text, S. I., & Instruments, A. (2009). Supporting Information, 1–7.

Theobald, J. C., Duistermars, B. J., Ringach, D. L., & Frye, M. a. (2008). Flies see second-order motion. *Current biology : CB*, *18*(11), R464–5. doi:10.1016/j.cub.2008.03.050

Tuthill, J. C., Chiappe, M. E., & Reiser, M. B. (2011). Neural correlates of illusory motion perception in Drosophila. *Proceedings of the National Academy of Sciences of the United States of America*, *108*(23), 9685–90. doi:10.1073/pnas.1100062108

Van Lutterveld, R., Diederen, K. M. J., Koops, S., Begemann, M. J. H., & Sommer, I. E. C. (2013). The influence of stimulus detection on activation patterns during auditory hallucinations. *Schizophrenia research*, *145*(1-3), 27–32. doi:10.1016/j.schres.2013.01.004

Venken, K. J. T., Simpson, J. H., & Bellen, H. J. (2011). Genetic manipulation of genes and cells in the nervous system of the fruit fly. *Neuron*, *72*(2), 202–30. doi:10.1016/j.neuron.2011.09.021

Wang, Z., Pan, Y., Li, W., Jiang, H., Chatzimanolis, L., Chang, J., Gong, Z., (2008). Visual pattern memory requires foraging function in the central complex of Drosophila, 133–142. doi:10.1101/lm.873008.4

Webb, B. (2002). Robots in invertebrate neuroscience. *Nature*, *417*(6886), 359–63. doi:10.1038/417359a

Wessnitzer, J., & Webb, B. (2006). Multimodal sensory integration in insects--towards insect brain control architectures. *Bioinspiration & biomimetics*, *1*(3), 63–75. doi:10.1088/1748-3182/1/3/001

Wilkinson, M. (1997). Nonlinear dynamics, chaos-theory, and the" sciences of complexity": their relevance to the study of the interaction between host and microflora. *Old Herborn University Seminar Monograph*, (1984), 1–17. Retrieved from http://iwi138.iwinet.rug.nl/informatica/users/michael/nonlin96.pdf

Wolf and M. Heisenberg. (1984). *Studies of Brain Fuction: Vision in Drosophila. Springer-Verlag* (Vol. 12). Berlin Heidelberg New york Tokyo: Springer -Verlag.

Wolf, R, & Heisenberg, M. (1980). Drosophila melanogaster, *80*, 69–80.

Wolf, Reinhard, & Heisenberg, M. (1991). Basic organization of operant behavior as revealed in Drosophila flight orientation, 699–705.

Wu, C. F., & Pak, W. L. (1975). Quantal basis of photoreceptor spectral sensitivity of Drosophila melanogaster. *The Journal of general physiology*, *66*(2), 149–68.

Wyman, J. (2013). Motor outputs of giant nerve fiber in Motor Outputs of Giant Nerve Fiber in Drosophila, 405–421.

Zhou, Y., Ji, X., Gong, H., Gong, Z., & Liu, L. (2012). Edge detection depends on achromatic channel in Drosophila melanogaster, 3478–3487. doi:10.1242/jeb.070839

8. ACKNOWLEDGEMENT:

I give immense gratitude for my guru and great companion, Prof. Björn Brembs, for offering me the opportunity to undertake a Ph.D. program in his laboratory. During my difficult times, his support was invaluable and timely. He understands the psychology of foreign students and he never stopped encouraging me to apply my talents to the research environment. We enjoyed wonderful times during scientific travels around the world and I learned a great deal about the global research culture. For this reason, I am deeply grateful for the training opportunity he offered me. Our daily lab lunch at 11.30 AM significantly changed my attitude towards the research lifestyle. It was a great pleasure to be part of the research environment that Björn created in Berlin. Our weekly lab meetings shaped my research project tremendously, and he had a great deal of patience with my research outcomes. I am, I have been, and I shall always be grateful to him.

Dr. Julien Colomb, who was a great mentor and highly supportive during my entire training period. His teaching methods are revolutionary, and impacted the way I approached my project. I extend my gratitude and wish him to pass on his invaluable support to future students. I am thankful to Ms. Hopp who had great patience and time to teach me standard fly techniques. It is a pleasure to state that she is the first German women I have met in my life. My fellow colleague Chrisi was also very kind and helpful throughout my time in the laboratory. I am grateful for the time it took for her to teach me Bavarian culture. I want to also thank Konstantin Lehmann for his valuable time during our discussion on advanced computing techniques and his assistance while I was in Berlin. I also want to take this opportunity to thank Prof. Nawrot and Jan Soelter for teaching me the Matlab course during 2010, which helped me make significant progress in my project. I want to thank katrin Barbara for the time we spent during our conference visits and valuable suggestion on my thesis. My special thanks to my friend Rio T with whom I had wonderful time in the summer.

It was a great pleasure to have Ramesh, Jaime, Rio, Sheriff, Neil Jin, Yan Dyck, Devrim, Clelia, Mano chitra, Yuva, Vinodh, Saroja, Wengui, Eswari, Maggie, etc. as friends and I appreciate their time listening to my artful theories and speculations. Undoubtedly, I am happy to have met every one of them during my time in Berlin. Above all, I have no words to express my feeling towards my 'Raja' family. They gave me immense hope during my difficult times and never failed to encourage me. My brother MathanK deserves the highest level of compliments for his extensive support and time. I am very thankful to all the readers who took the time to read my entire thesis.